THE CURRENTS OF PENOBSCOT BAY, MAINE:
Observations and a Numerical Model

by
Halsey R. Burgund

Advisor: Philip Bogden
2nd Reader: George Veronis
April 21, 1995

A Senior Thesis presented to the faculty of the Department of Geology and Geophysics,
Yale University, in partial fulfillment of the Bachelor's Degree.

The Currents of Penobscot Bay, Maine: Observations and a Numerical Model

Abstract

This paper provides an investigation of the physical oceanographic characteristics of Penobscot Bay, Maine. Penobscot Bay is one of the largest estuaries on the Maine coast, extending nearly 65 km from the Penobscot River in its northeastern corner to the Gulf of Maine to the south. The bay is a vital part of the area's economy, providing shipping channels and biological resources. This study is comprised of two parts, the first being an observational field study and the second being a 2-D numerical model of the bay which investigates both tidal and non-tidal currents.

The field work was done throughout the summer of 1994 and included a drifter study and a hydrographic survey. Drifters were designed and built specifically for this project, and a technique for tracking the drifters visually using a power boat and a hand-held GPS unit was developed. Eight drifter surveys were completed. The results shed light on several general trends occurring in the bay, but were not extensive enough to yield conclusive information about the overall circulation patterns.

The hydrographic survey was done over the course of two days in early July using a Seacat CTD. Close to 100 casts were made in both the eastern and western portions of upper Penobscot Bay, giving a hydrographic picture of the bay in mid-summer.

The second part of this paper is a 2-D numerical model. The finite difference model solves the vertically integrated equations of motion for a homogeneous fluid in a rotating reference frame. The equations are simplified by neglecting non-linear terms. The model is implemented incorporating the actual bathymetry and topography of Penobscot Bay. The model was first run with an M2 tidal signal as forcing at the open boundary in order to understand the tidal current field.

Three non-tidal currents, forced by a tidally averaged vorticity flux, wind stress, and river outflow, were investigated also. From the linear tidal solution, the tidally averaged vorticity flux was calculated and then used to force the model. Uniform wind stress and river outflow were also used to force the model.

The tidal solution showed currents on the order of 50 cm/s flowing into and out of the bay with a greater magnitude near the open boundary. Sea surface height was magnified at the head of the estuary. The tidally induced residual flow field was characterized by several near land regions of greater flow magnitude on the order of 10 cm/s. Wind stress generated currents of this same magnitude which were characterized by "with wind" flow in the shallower areas and "against wind" flow in the deeper areas. River outflow currents were an order of magnitude smaller than the other non-tidal currents, flowing south around the islands. The tidal currents are dominant, although wind driven and vorticity flux induced flow are shown to play an important role in the non-tidal circulation in Penobscot Bay.

INTRODUCTION:

Penobscot Bay is one of the largest estuaries on the coast of Maine extending close to sixty five kilometers from the mouth of the Penobscot River southwards to where it opens into the Gulf of Maine (see figure 1.1). The lower Penobscot Bay topography is complicated by several large islands and a multitude of smaller ones. The upper bay is simpler in that it is neatly divided into eastern and western channels by Islesboro Island, a large island which runs north/south down the center of the bay (see figure 1.2). The bay ranges in depth from 100 m nearer the Gulf of Maine to 20m in the northern bay between Islesboro and Sears Island.

Penobscot Bay has been polluted over the years by many different sources. The bay is a well trafficked body of water, being used for commercial fishing and oil transport as well as providing a beautiful area for pleasure boating during the summer. In addition to the boating activity on the bay, there are several paper and textile mills which discharge their effluent into Penobcsot River. Sewage discharge from 12 communities is also dumped into the river (Haefner, 1967). It is of vital importance to understand the currents, both tidal and the residual, in the estuary, and the hydrography of the estuary, in order to control this pollution so as to preserve the biological and chemical system of the bay.

The currents in Penobscot Bay, as in many estuaries, are dominated by the tides, the wind, and the fresh water outflow from the Penobscot River (Normandeau, 1975). The tides in the area range from 2.3-4.2 meters between high and low water at neap and spring tides respectively (Normandeau, 1975). The dominant tidal component is the M2 with a period of 12.4 hours. The winds are variable depending on the weather patterns that pass through the area, but there are some general seasonal shifts of wind direction. In the summer, when the data for this study was collected, the prevailing winds are from the south/southwest. In the winter months, however, the winds shift and blow out of the north/northwest (Normandeau, 1978). The outflow from the Penobscot River is also seasonally variable. The maximum monthly outflow generally occurs in April or May due to spring snow melt, and there is a secondary late fall maximum in November. Minima, when the outflow is as low as one third of the maximum values, occur in February and September (Haefner, 1967; Normandeau, 1978). The mean daily outflow from 1950-60 as recorded by the USGS gauge at West Enfield, Maine was 12,820 ft^3/s. It has been hypothesized that the water

generally flows up the estuary in a layer near the bottom and flows out of the estuary in a thin layer on top (Normandeau, 1975).

The intent of this study is to try to understand what the dominant forcings of the currents are, what the residual circulation pattern looks like, and to establish a general hydrographic picture of Penobscot Bay during the study period. An independent field project was undertaken, and the data collected was supplemented by previously collected data from other sources to provide the most comprehensive and unbiased view of Penobscot Bay. The second part of the study is a 2-D numerical model of Penobscot Bay. Both the tidal and sub-tidal currents are investigated using different forcing mechanisms. This model provides a different approach to looking at the currents in Penobscot Bay.

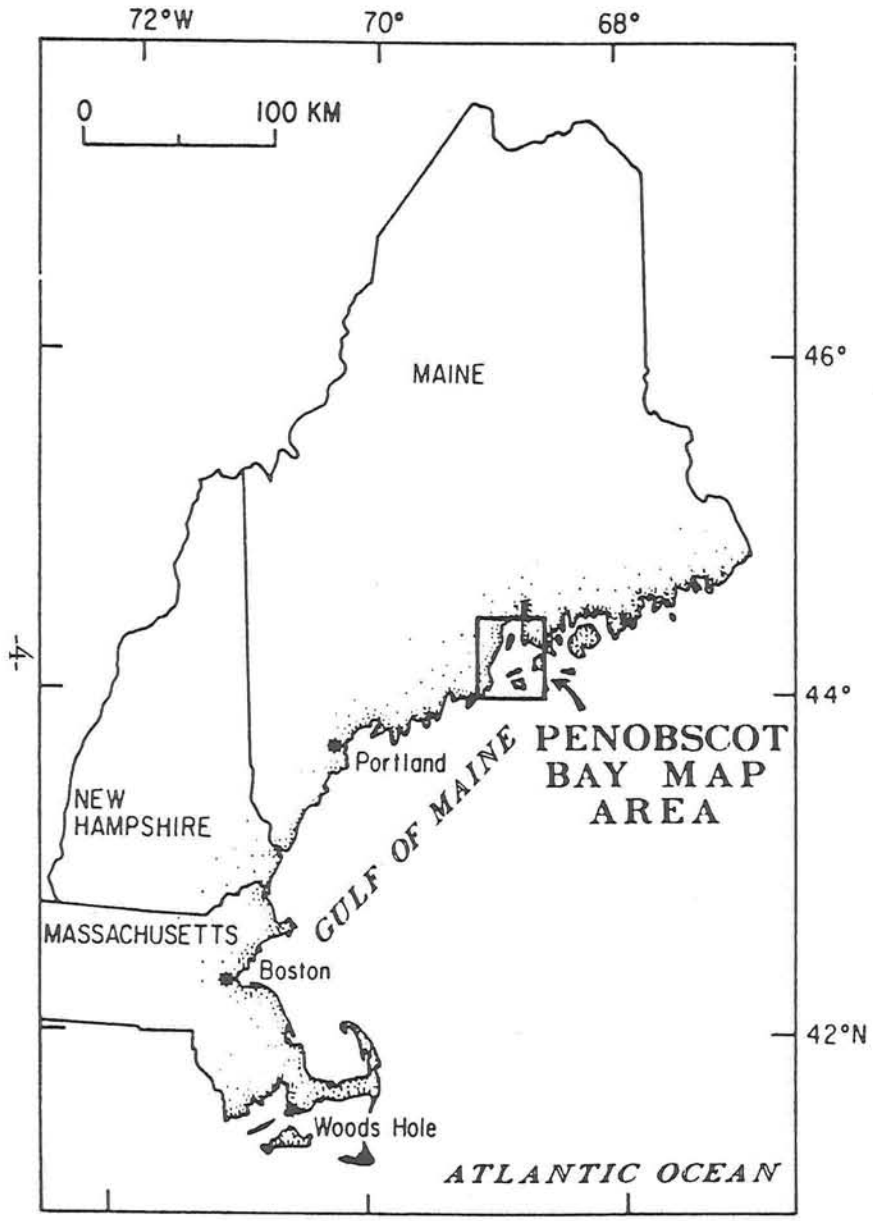

Figure 1.1

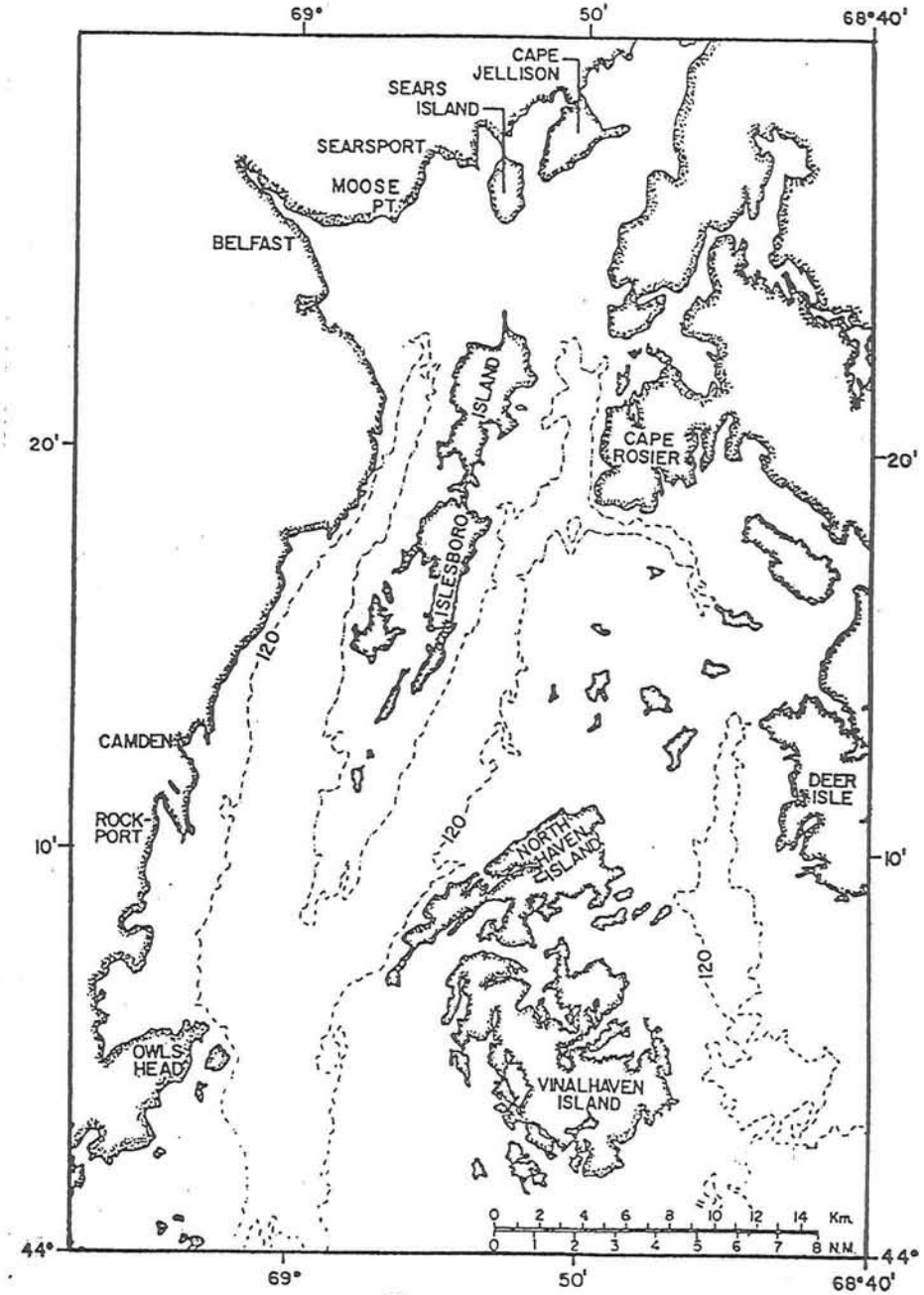

Figure 1.2

PART I: OBSERVATIONS

METHODS:

This project involved both the design and the implementation of a field study using both drifters and a CTD. The drifters were designed and constructed specifically for this project and a technique for tracking them was developed.

Drifter Design and Construction:

The drifters were designed to be easily assembled by hand and to have maximum performance for a minimum price. Therefore, they were constructed out of common household materials and were designed to leave room for modification during construction. The drifters were inexpensive, easy to construct, and effective in tracking surface currents.

The basic design of the drifter follows that of the Davis drifter (Davis, 1985). The drifter has four underwater sails at right angles to each other and a vertical pole acting as a central structural member. Contrary to the Davis drifters, which are tracked by radio, these drifters were designed to be located visually, requiring a flag on the central pole sticking two feet up above the surface of the water. The flags were bright orange or yellow to make them easy to spot on the water from a distance. Unfortunately, they were still hard to spot due to waves, fog, and similarly colored lobster pots.

The drifters were designed to follow as closely as possible the movement of surface water parcels in its vicinity. Therefore, they were designed to have a maximum amount of underwater drag and a minimum above water drag. The underwater sails provided underwater drag, and the thin vertical pole and flag provided minimal above water drag. Minimal above water drag was essential because if the wind directly pushed the drifter, the drifter trajectory would no longer accurately represent the trajectory of a parcel of surface water. The drifters do not, however, completely disregard the wind in that they do track wind-driven currents, just not the wind itself.

The frame and sails of the drifters were constructed from 1/2 inch electrical conduit PVC pipe and blue plastic tarpaulin material. The PVC was chosen because it

is cheap, easy to cut, and light. The tarp worked well because it doesn't absorb water and is also easy to work with. The sails were 30 cm. wide and extended 50 cm. down into the water column. The drifter sails were held in position at their top edge by a cross of PVC pipe, in the center, by the vertical flag pole, and on the outer edge by a hanger bent around the PVC. It wasn't necessary to frame the bottom edge because the sails stayed in position without any framing. Please see figure 1.3 for drifter diagram.

Flotation and stabilization for the drifters was provided for by Styrofoam billet material and lead fishing weights. Davis (1985) recommends that four separate flotation devices attached to the end of the four arms of the drifter be used rather than a single central flotation collar. This advice was taken and each drifter was fitted with four pieces of the billet material attached to the end of each arm. 18 oz. of fishing weights were attached to the lowest central point of the drifter to keep it upright in the water. In order to reduce windage, the floats were trimmed down so that they floated three quarters in the water and one quarter above. Each drifter was tested with only three of its four floats to ensure that it would not sink in the event it lost one float due to a collision with a boat or any other extraneous circumstance.

One drogued drifter was built. It was designed to track the currents at a depth of ten meters. The design was similar except no flotation was attached to the sail unit and a pole with a flag and floatation was attached to this unit with a ten meter piece of line. The sail unit then was weighted accordingly and it sunk to ten meters leaving the flag standing at the water's surface (see figure 1.4).

Eight drifters were constructed for this project. They were individually numbered and marked with my name, phone number, and address so if any were lost they could be returned and used again, and long term data could be obtained.

CTD Data Collection:

A Seabird Seacat hand held CTD was used for two hydrographic surveys in both East and West Penobscot Bays. The first survey was done in the West Bay on July 5th during the latter half of a flood tide. The second survey on July 6th included both bays encompassing a flood tide in East Bay and a slack tide in West Bay. See figures 1.5 and 1.6 for the locations of the transects and individual CTD casts for each survey.

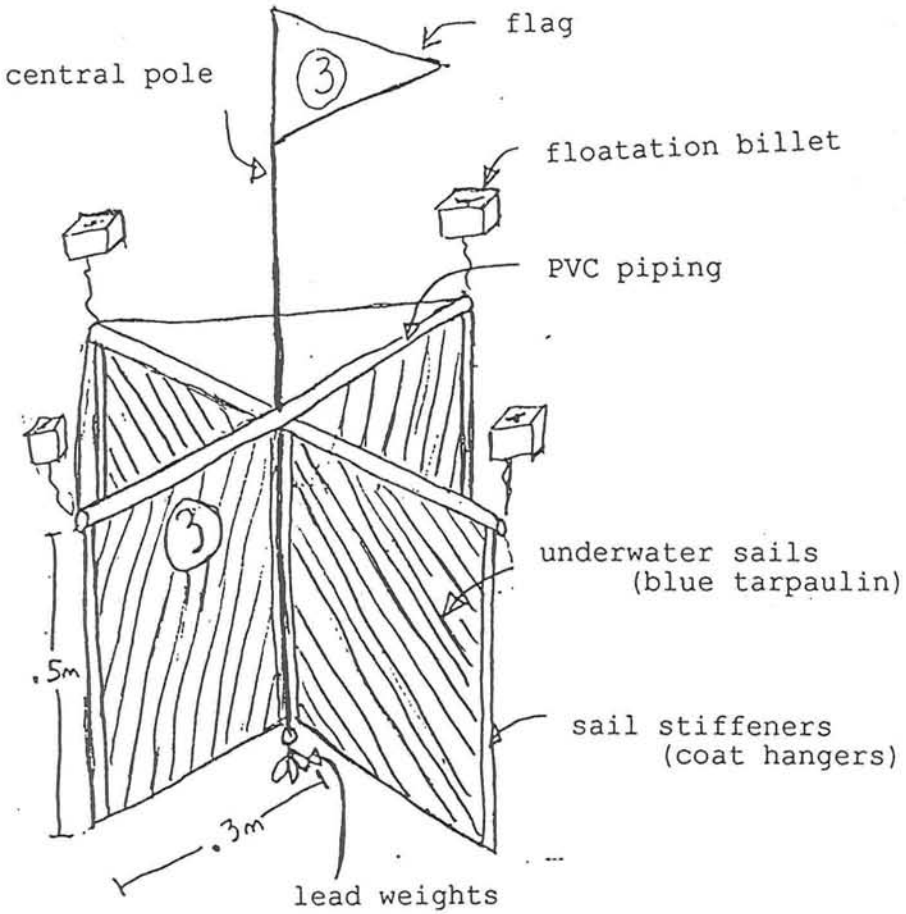

Surface Drifter Design

Figure 1.3

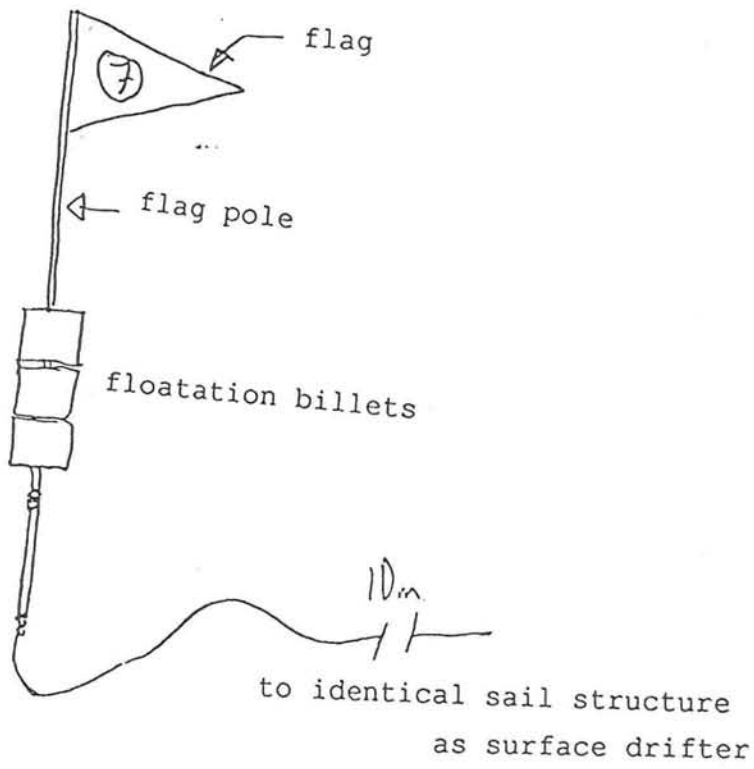

Drogued Drifter Design

Figure 1.4

CTD Transects - July 5th, 1995

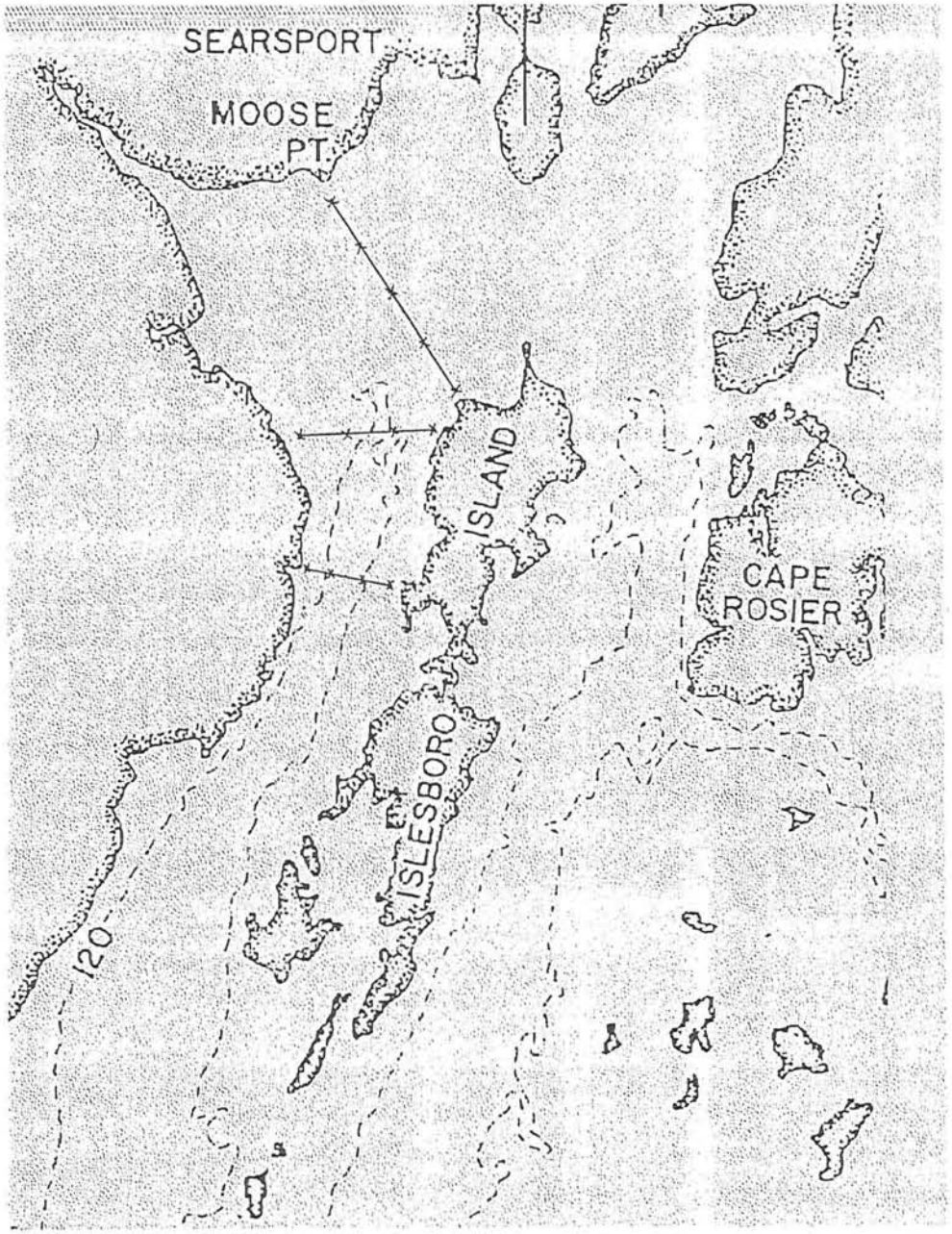

Figure 1.5

CTD Transects - July 6th, 1995

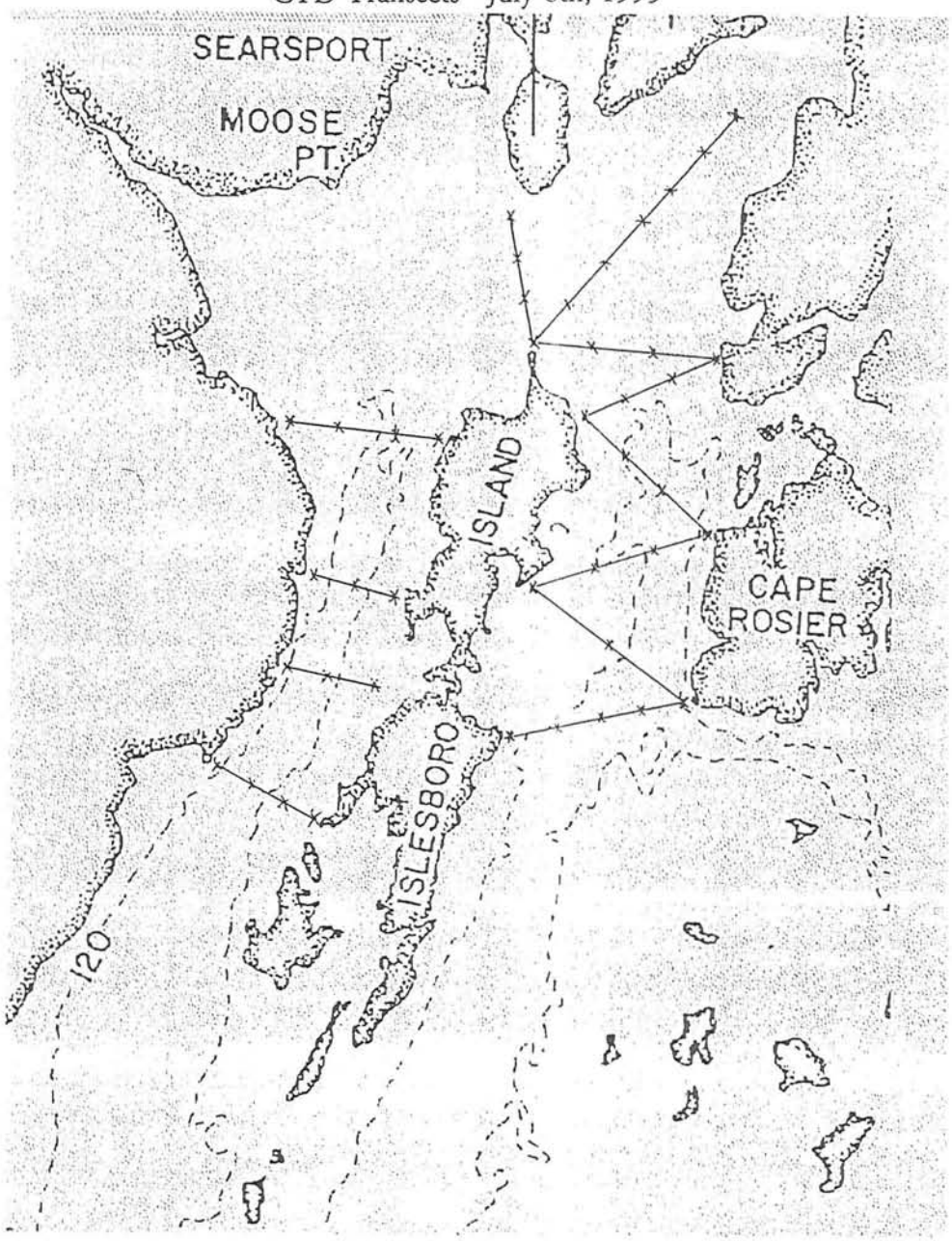

Figure 1.6

CTD data was collected by stopping the boat on station and lowering the CTD over the side of the boat. The CTD is held at the surface of the water for about one minute to let its sensors equilibrate and then it is lowered at a constant rate until it hits the bottom at which point it is pulled up. As the device passes down through the water column it records conductivity, temperature, and depth/pressure every half second. This raw data is stored in an internal recording device and memory unit and then downloaded to a portable PC after 15 or so long casts to ensure that no data is lost. The CTD is then re-initialized and ready to record more data.

The CTD data is a helpful supplement to the drifter data as it will provide a picture of the hydrographic structure of the bay which can affect the surface currents. Figures 1.25 and 1.26 are examples of the profiles that the CTD yields. Figure 1.25 shows a station just west of the northern tip of Islesboro, and figure 1.26 shows a station in the east bay, closer to the southern portions of Islesboro.

Drifter Field Work:

A total of eight drifter surveys were done; six full tidal cycle surveys and two half tidal cycle surveys. The tidal cycle surveys were intended to cover all of upper Penobscot Bay in both East and West Bays. In these surveys two, three, or four drifters were dropped off at a predetermined location(s) and were subsequently located every hour and a fix was taken with a hand held GPS unit to determine the exact position of the drifter. This was done for 13 hours to ensure that a full tidal cycle was included in the data set. All of these surveys were begun around five o'clock in the morning so that it would remain light out during the entire survey.

Survey #1 was mainly in the north western part of the bay. Four drifters were deployed in two pairs separated laterally in the bay. Survey #2 was in the East Bay and again involved four drifters in two pairs deployed with lateral separation. Only three drifters were deployed in surveys #3 and #4, and they were deployed all at the same location. They did separate, but not enough to gain the same separation as the other two surveys. The decision to deploy only one group of drifters was based on the difficulty encountered in locating the drifters and the subsequent loss of three of the eight drifters. Survey #5 was similar to #1 and #2. Survey #6 was partially stymied by fog so that only two drifters at one location were deployed and tracked.

Figures 1.8 through 1.13 show the drifter trajectories for the individual surveys. These are preliminary plots from the raw data and give a picture of what the drifters did throughout the tidal cycle in different parts of the bay. Latitude minute markings

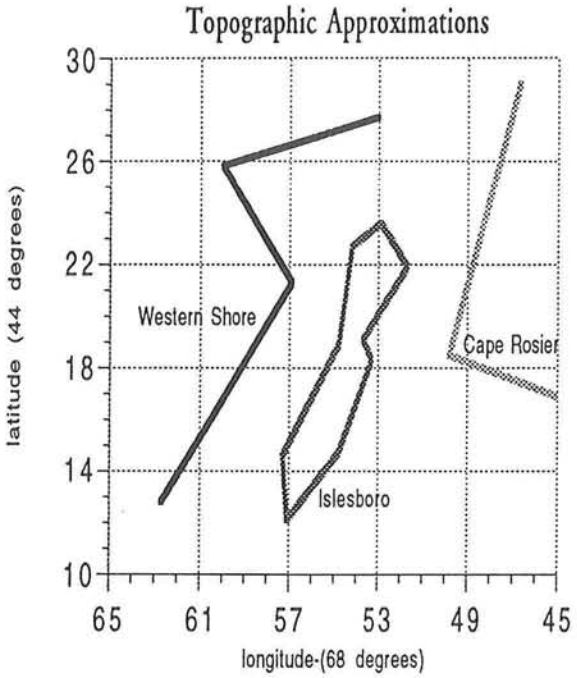

Figure 1.7

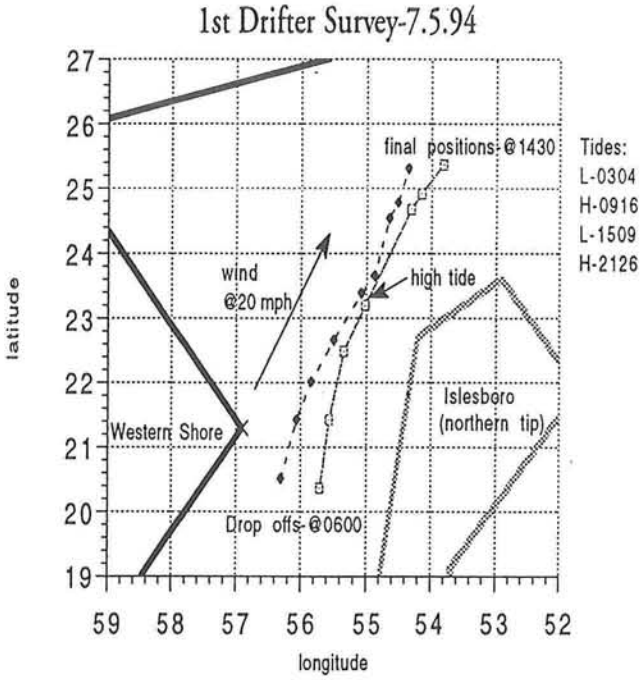

Figure 1.8

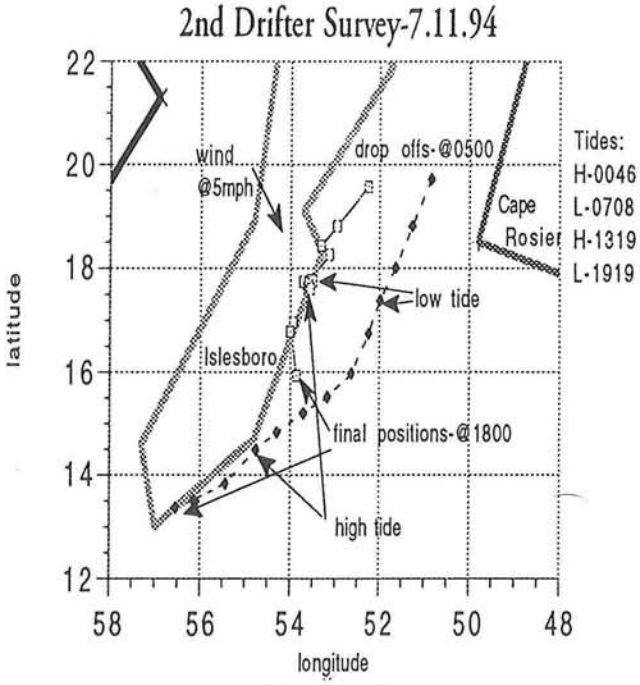

Figure 1.9

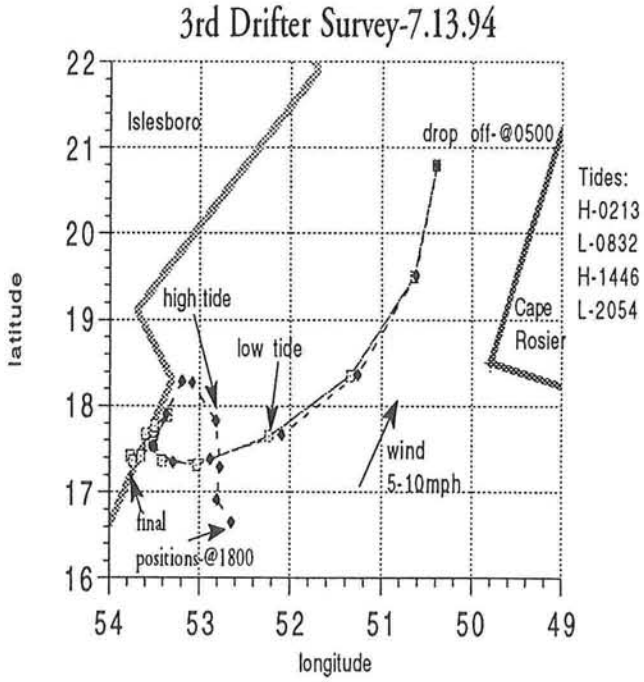

Figure 1.10

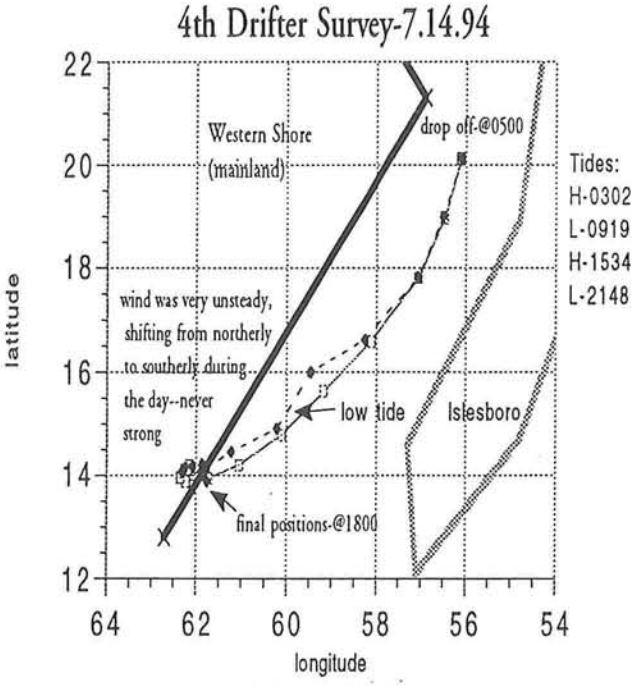

Figure 1.11

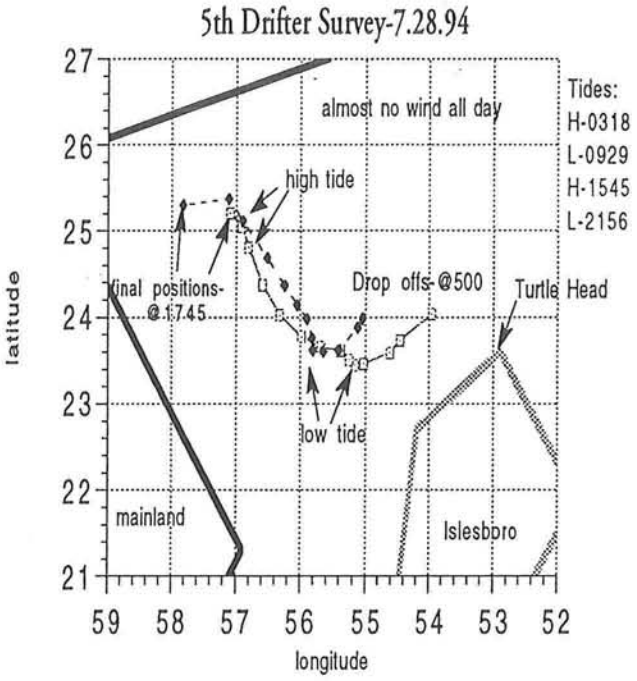

Figure 1.12

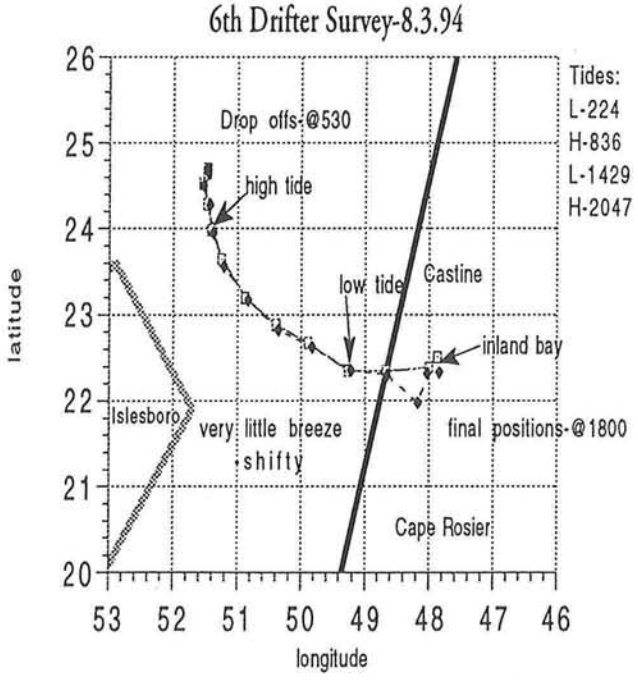

Figure 1.13

above 60 should be considered the next degree. The land masses drawn on the diagrams give the approximate positions of Islesboro Island and the eastern and western shorelines to give the reader a general idea of where each survey took place. These are shown in figure 1.7.

The half tidal cycle surveys were of another type. These were redeployment surveys in which several drifters were deployed, tracked for a few hours, and then picked up and redeployed at their initial deployment locations. The point of this type of survey was to look at the evolution of the velocity field in a certain area over a portion of the tidal cycle. Two of these surveys were done, both in the East Bay near the 44° 21' line of latitude. In both surveys, four drifters were tracked, three surface drifters and one drogued drifter which measured the current at a ten meter depth. In the first survey, two drifters were deployed near the western part of the bay and two, including the drogued drifter, nearer the central portions of the bay. Both pairs were tracked for two hours at a time and were redeployed twice giving three separate trajectories for each drifter over a six hour period. The second redeployment survey was different in that two drifters were dropped individually in the western and central portions and a pair, again including the drogued drifter, was dropped near the eastern boundary. This time the drifters were tracked for three hours at a time and only redeployed once yielding two trajectories for each drifter. Selected plots of this data can be found in figures 1.14 and 1.15.

The three drifters that were lost during surveys were all returned because of the information written on them. These drifters yielded general, and unfortunately sparse, long term circulation data because the last seen position and the found position are known as well as the time lost. Nothing, however, is known about the path the drifters took from initial to final position.

RESULTS:

The following discussion is of both the results collected in this study and the results of other physical oceanographic studies run in Penobscot Bay in the past. A comparison and assimilation of all results is presented also.

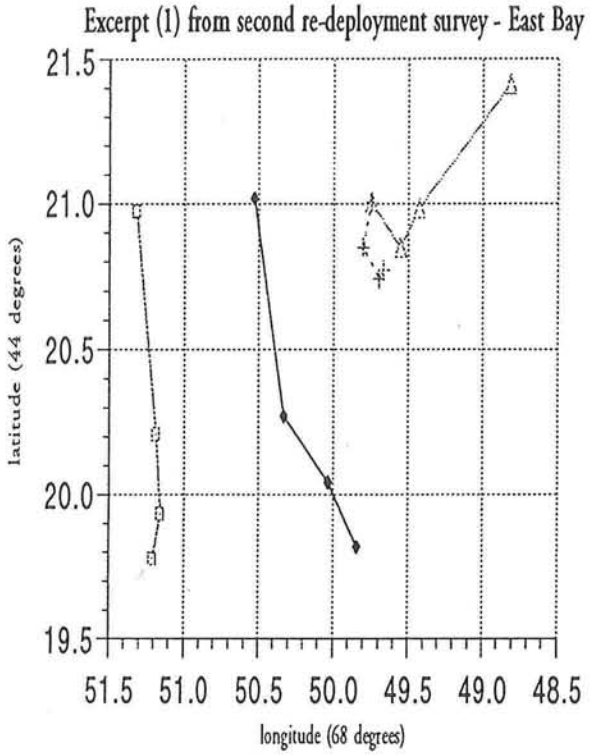

Figure 1.14

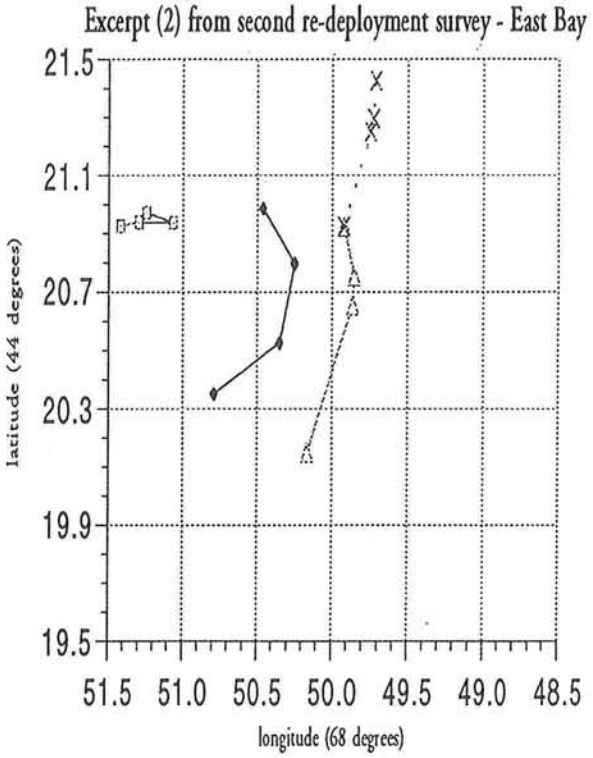

Figure 1.15

Current Data:

Summary of Previous Work:

Current data has been collected by Normandeau Associates (1975) in their environmental survey of 1975 and by NOS/NOAA in 1969-70. The NOAA data has been used by Humphreys and Pearce (1981) to verify their 3-D numerical model of the bay. The Normandeau data is both Lagrangian and Eulerian in that both drifters and moored current meters were used. The NOAA data set consists of data solely from fixed point current meters.

The Normandeau report provided an extensive data set of current strength and direction for four stations in northern Penobscot Bay at different stages of the tide, but provided only weak evidence hinting at a 2-D residual circulation pattern. At high tide there were weak north/northeast flows (.08 m/s) in both the top and bottom layers. At mid ebb the flows were consistently southwards, down estuary, and were considerably stronger than those at high tide (.2 m/s). Data from low tide showed weak northward flow in the west channel and south/southeast flow in the central and eastern portion of northern Penobscot Bay in both the surface and bottom layers (.1 m/s). At mid flood flows were towards the north/northeast. Surface flows of .2 m/s were stronger than the .15 m/s bottom flows but were in the same direction.

This quantitative data, represented by rose diagrams in the Normandeau report, can be averaged over the entire tidal cycle in order to get a first order picture of the net tidal drift. The results of this analysis show that the general pattern for both the surface and the bottom water is to flow northwards in the west bay, eastwards in the northern sections, and then southwards in the east bay. This is suggestive of a clockwise circulation around Islesboro Island, although the evidence is sparse. The station in the mouth of the river acts as somewhat of an anomaly in that the surface and bottom flows are in opposition and are directed into and out of the river. This is possibly a density driven effect created by the river outflow.

The Lagrangian data was collected by the use of surface floating drift cards in a later study (Normandeau, 1978). In the first study, 300 drift cards were deployed by helicopter at different locations throughout the bay on a specified day. The cards which were found and returned to Normandeau suggested the same residual circulation as stated above; clockwise around Islesboro. Drift cards deployed in the eastern bay were generally recovered south of their drop off location whereas drift cards deployed in the west bay were generally found north of where they were

dropped off (see figure 1.16). Normandeau suggests that the cards in the west bay moved north as a result of wind stress but the cards in the east bay moved south under the influence of the river. No tidally rectified residual current was proposed. A second drift card study was done in which drift cards were time-released from a single location over an entire tidal cycle. The result was a consistent northerly motion (see figure 1.17). This drift pattern is suggested in the report to be mainly a reflection of the wind patterns during the week long study period.

Another study in Normandeau (1978) was vaguely suggestive of the same clockwise circulation around Islesboro. In this report, tidally averaged net displacements were calculated for northern Penobscot Bay. In the northwest channel, the surface net drift was 2.1 km to the north over a tidal cycle. In the north bay, the drift was of the same magnitude but towards the east/southeast. The bottom net drifts were generally towards the east throughout the northern bay, but were weaker than the surface motion. This study was not overly comprehensive and was only done once, so the results cannot be weighed heavily.

The NOS/NOAA data was collected by current meter arrays for a two week period in early summer of 1970. Humphreys and Pearce (1981) generated plots of the residual currents at different depths using a progressive vector plot on this data. The resultant vectors are shown in figure 1.18. The speeds of the residual currents are from 1-6 cm/s and are generally oriented down estuary in the upper layer and up estuary in the lower layer. This two-layer circulation does agree with the two-layer pattern hypothesized in the Normandeau report, but no firm residual picture was established from this data or from the numerical model contained in the same paper. This two layer circulation is also a standard and expected estuarine circulation.

Results of the Field Project:

The results from the eight drifter surveys done in this study are shown in figures 1.8 through 1.15. This is the raw data, and simply shows the drifter trajectories for each of the surveys. The times of high and low tides are indicated on the plots. The first feature that one notices about these diagrams is that although the drifters were in general tracked for an entire tidal cycle, the typical tidal excursion ellipse is not seen. The drifters tended to move in one direction either up or down estuary during the entire tidal cycle rather than moving up estuary with the flood tide, reversing direction at high tide, and then moving down estuary during the ebb. This immediately indicates that the tides are not the only driving force behind the currents,

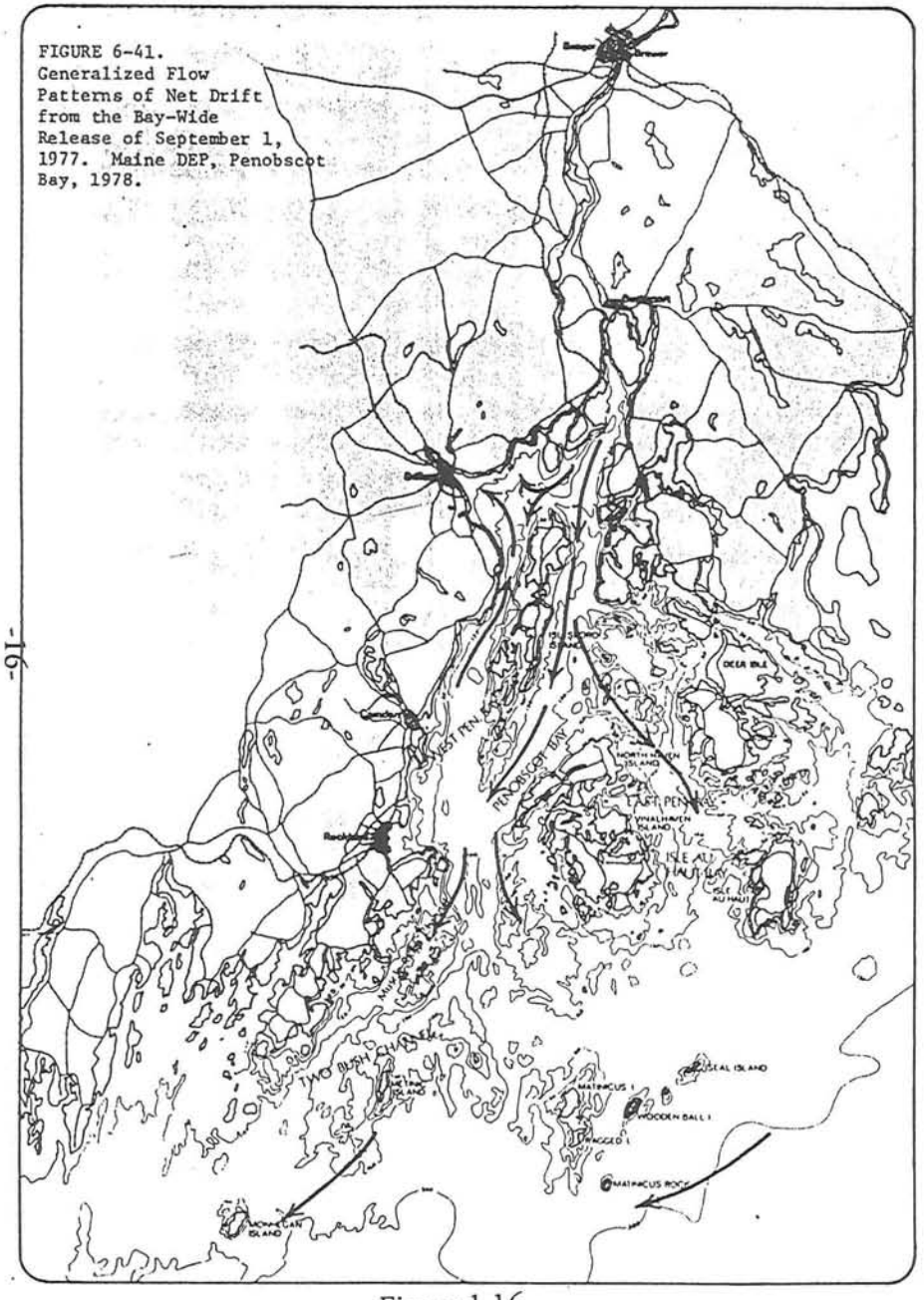

FIGURE 6-41.
Generalized Flow Patterns of Net Drift from the Bay-Wide Release of September 1, 1977. Maine DEP, Penobscot Bay, 1978.

Figure 1.16

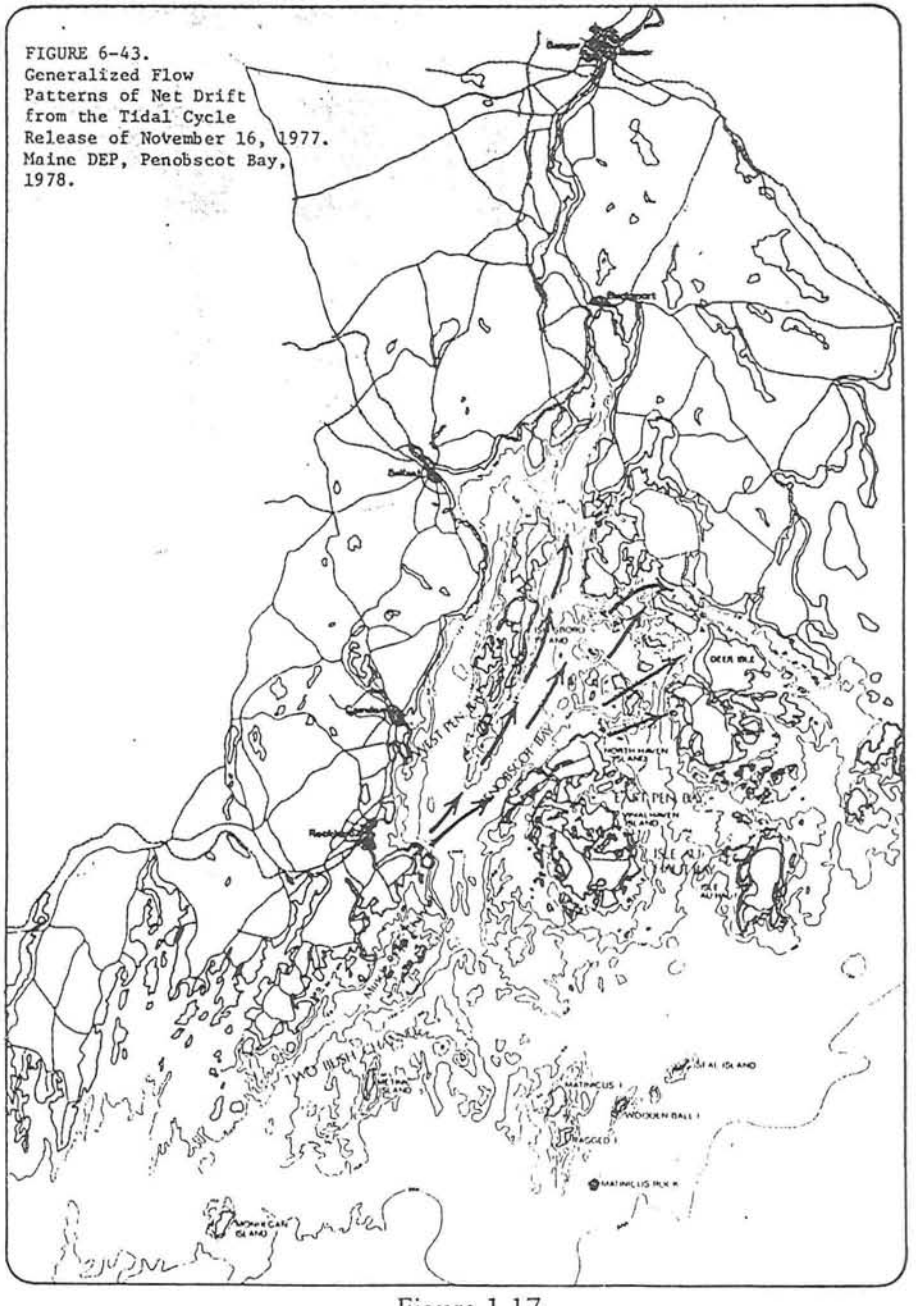

FIGURE 6-43.
Generalized Flow Patterns of Net Drift from the Tidal Cycle Release of November 16, 1977. Maine DEP, Penobscot Bay, 1978.

Figure 1.17

Net Drifts at Four Depths
(from Humphreys and Pearce)

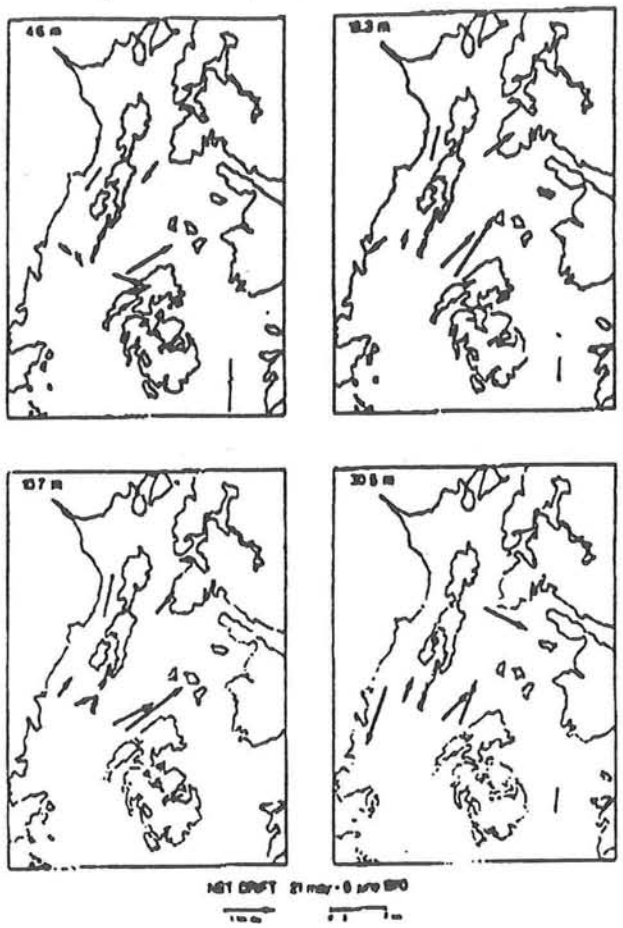

Figure 1.18

but that the currents are effected strongly by some other forcing mechanisms. As stated before, these mechanisms are most likely wind and river outflow. Figures 1.14 and 1.15 show the results of the second re-deployment survey, the solid lines being surface drifters and the dashed ones being drogued drifters. From these plots, one can see that the currents tend to switch directions on the western shore of east bay before the eastern shore. Although the drogued data is sparse, in this survey, it appears as though the bottom layer currents are somewhat de-coupled from the surface layer at this location. The scarcity of this type of data makes it difficult to make any definitive statement about this phenomenon, though.

Figure 1.19 shows the velocity in and out of the bay plotted against phase of the tide in relation to low tide for all the drifter data collected regardless of the drifter's location. This plot does not include all the data collected. Data from locations very near shore was thrown out due to possible lateral boundary layer effects. No clear signal is shown in this plot, again showing that the tidal velocity signal is complicated by other factors. The topography and bathymetry of the bay could cause a plot of this type to screen the tidal signal. As one can see from this plot, the velocities range from 0 - .7 m/s which is in general agreement with the data presented in the literature discussed above.

Simple two and three parameter models were fit to the drifter data. The two parameter model included a tidal term and a mean flow term.

$$u_i = A\cos(\phi_i) + B \tag{1.1}$$

where A is the amplitude of the tidal signal, ϕ_i is the phase of the tide, and B is the magnitude of the mean flow term. The three parameter model added a wind stress term to the two parameter model.

$$u_i = A\cos(\phi_i) + B + C|w_i|w_i \tag{1.2}$$

C is the wind stress coefficient, and w is wind speed. A least-squares fit of the data, solving for the parameters, was used for both of these models. The details of this fitting method are discussed in Menke (1984).

Neither model represented the entire data set well, although certain sub-sets of the data were represented well with the three parameter model. Some general, trend-type information was gained from the experimentation with these models, though. The entire data set was not represented well by the two parameter model (see figure

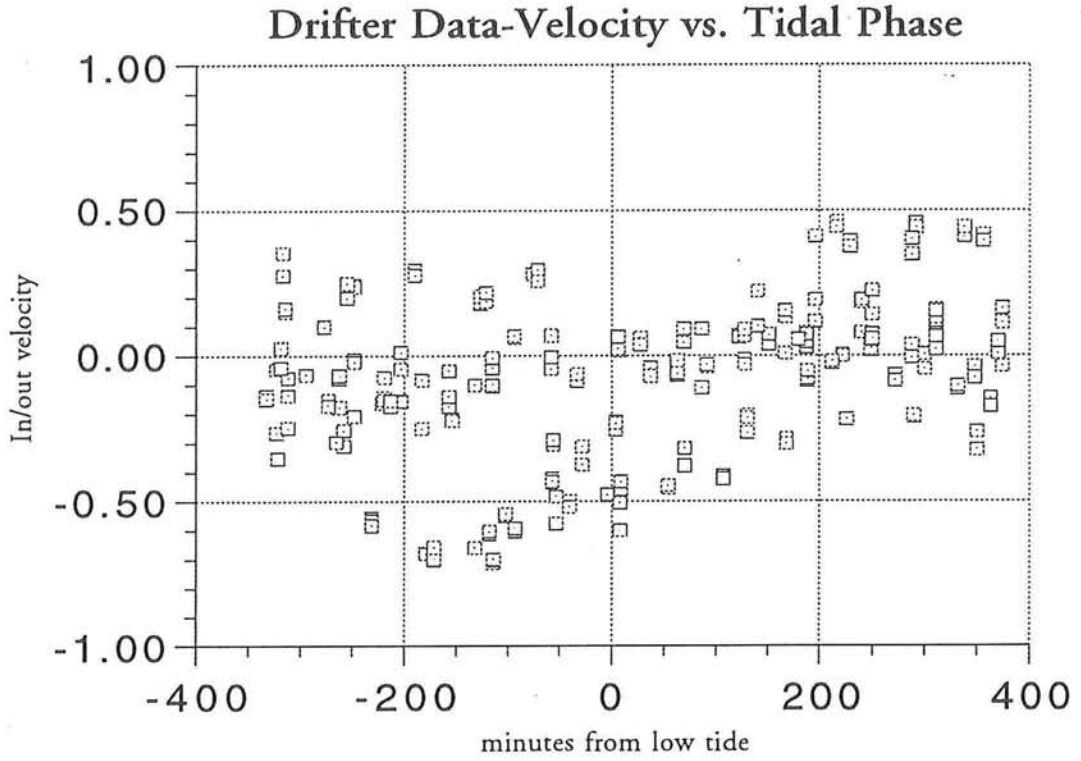

Figure 1.19

In/out velocity

Model Prediction

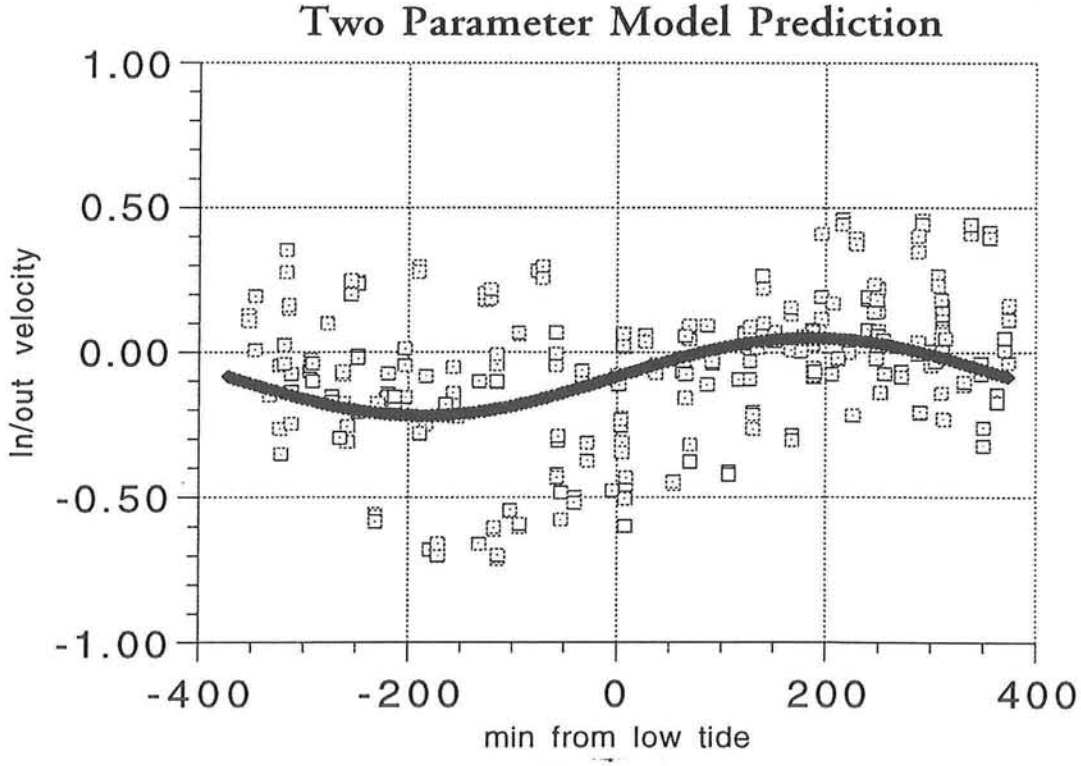

Figure 1.20

1.20). There existed too much scatter in the data for this type of model to even come close to representing a significant portion of it. But the addition of the wind term showed some improvement (see figure 1.21). Some of the scatter was taken into account by this term. This indicates that wind driven circulation is likely an important factor in the overall circulation of Penobscot Bay. The inadequacy of these models in fitting the entire data set is apparent from plots of the fit and from the plot of the difference between the data and the model prediction (see figure 1.22). Despite this, errors in the parameters for both models were calculated in order to quantify the accuracy of the fit. The errors in the parameters were on the same order of magnitude as the parameters themselves, indicating a low level of accuracy.

When the data was split up into individual surveys, the simple models fit the data more accurately. This is not surprising given that the number of points that the model was required to fit had been drastically reduced. For example, in surveys #1 and #6, the three parameter model predicted the drifter motion fairly well (see figures 1.23 and 1.24).

These simple models on the whole did not yield much useful information other than that the observed currents were considerably more complex than these models were capable of dealing with. The flow appeared to be not as strongly dominated by the tides as expected. Wind stress and some sort of mean flow, possibly river induced, were shown to be important in the current field of the study area. This mean flow was consistently negative (southwards) which supports the theory that it arises from river outflow.

HYDROGRAPHY:

The following is a discussion of the hydrographic data collected for this project as well as a summary of hydrographic data available in the literature. The intent of this section is to give an overall hydrographic impression of Penobscot Bay drawn not only from the field work done specifically for this project, but also from any other published hydrographic data collected in the bay.

Observations:

Penobscot Bay resides somewhere between the slightly stratified and the highly stratified estuary in the summer months according to the classification system proposed by Stommel (Pickard and Emery, 1982). The hydrographic data collected

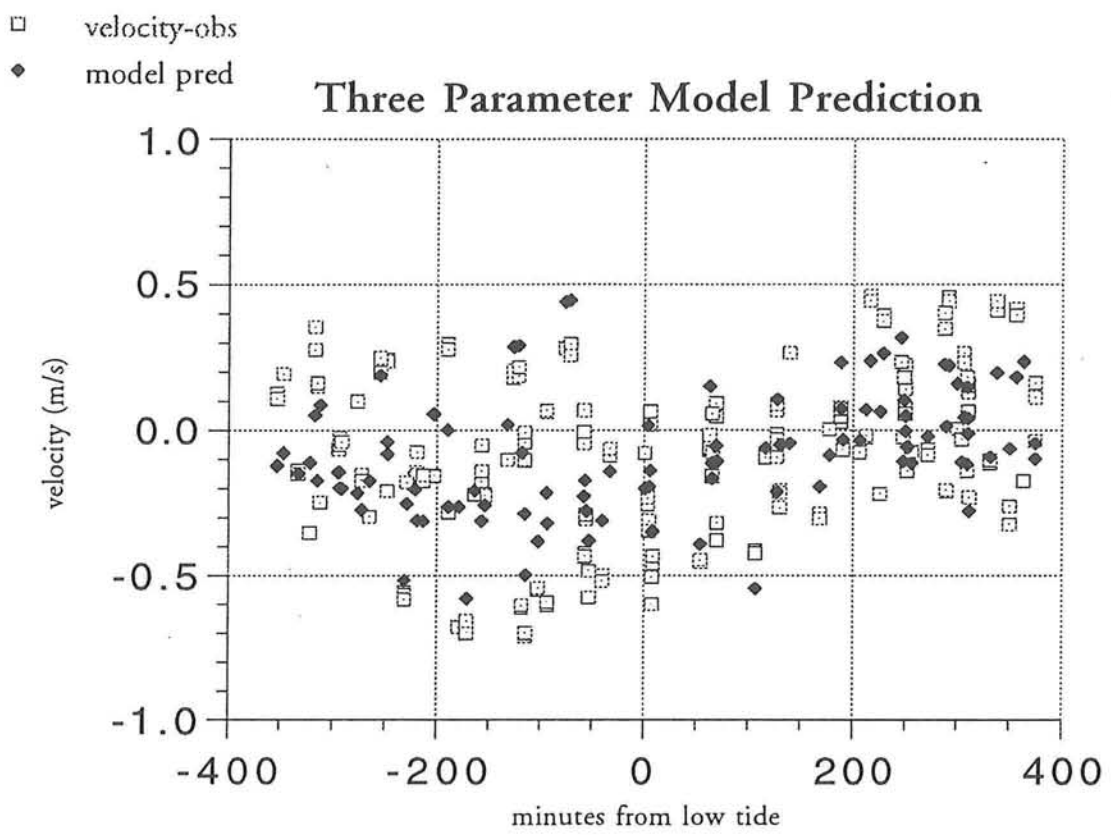

Figure 1.21

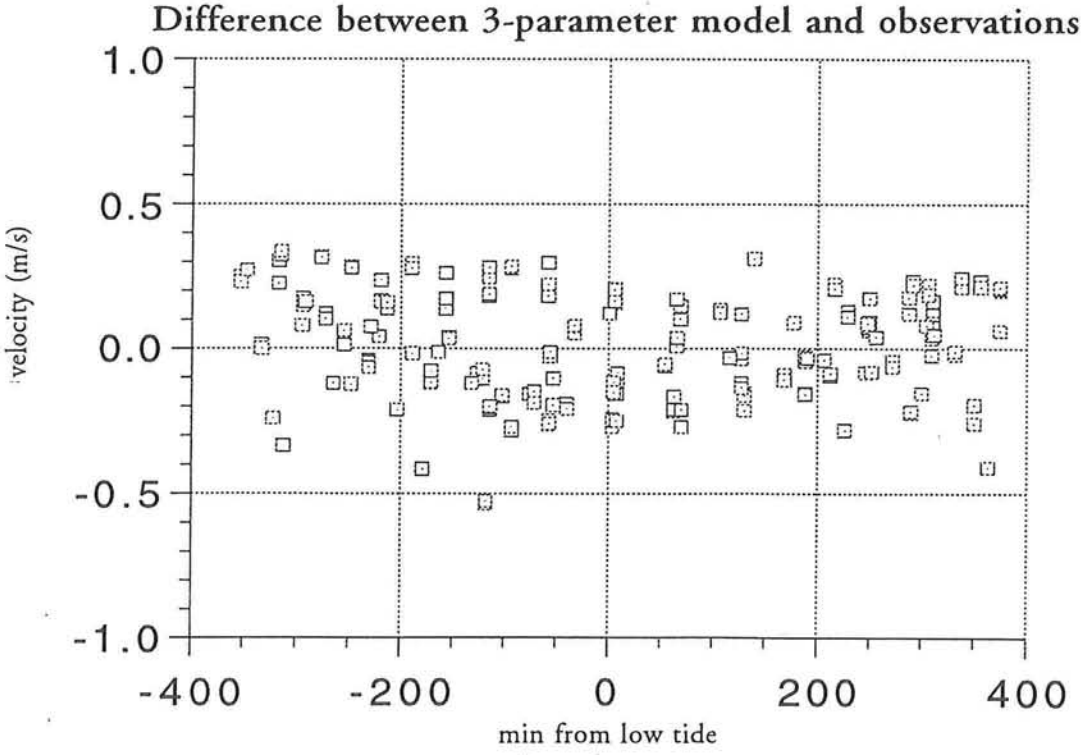

Figure 1.22

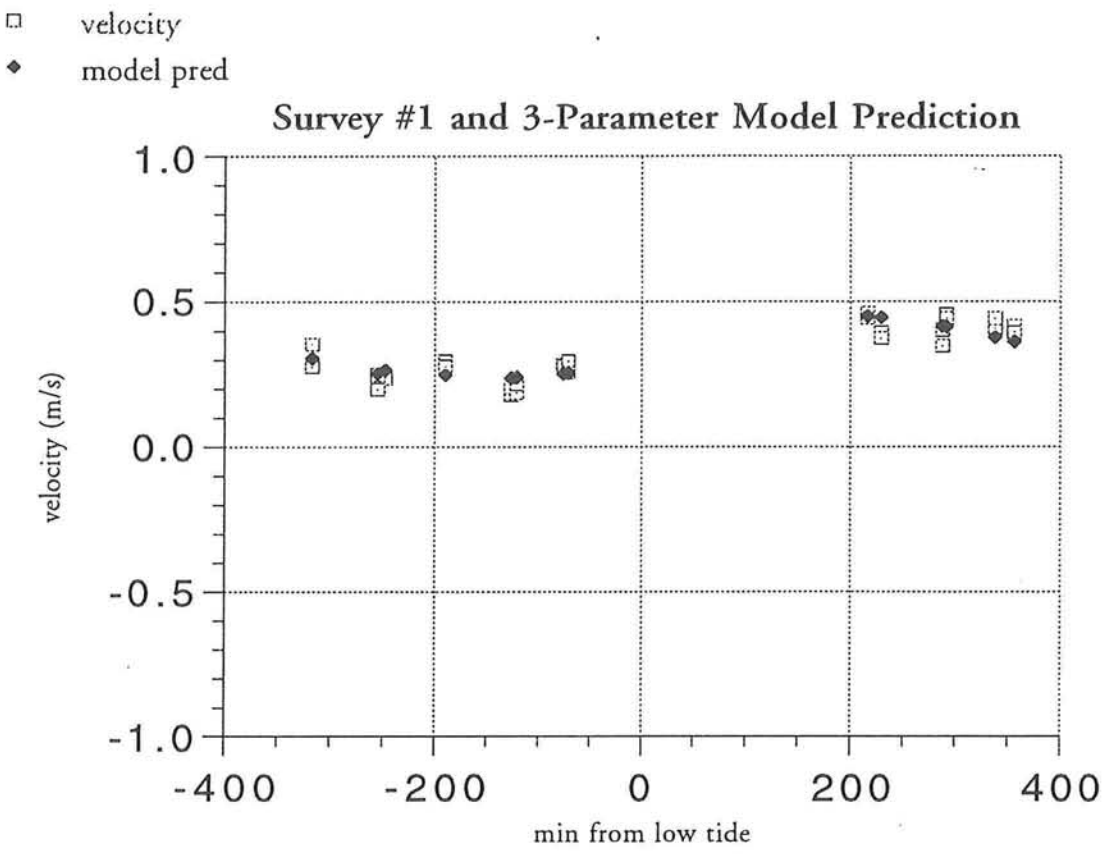

Figure 1.23

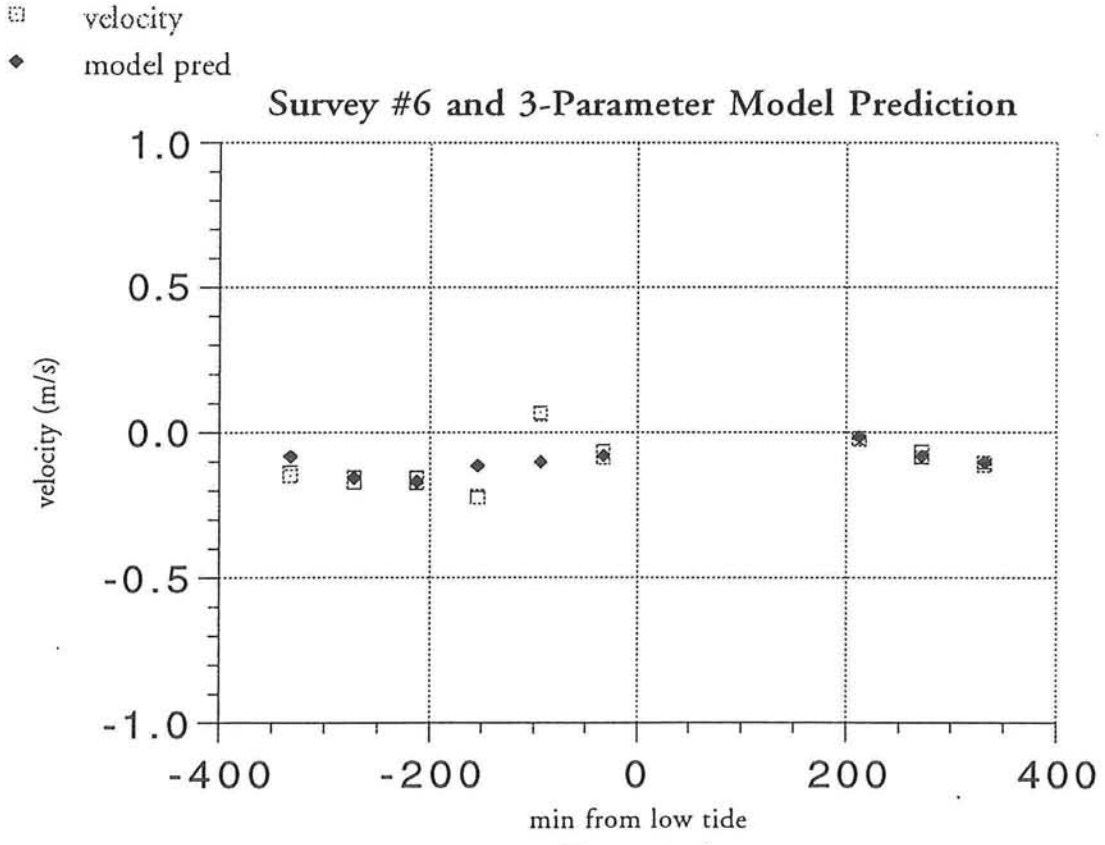

Figure 1.24

in Penobscot Bay shows that the bay exhibits a two layer system with less saline, warmer, and hence less dense water in an upper layer, and more saline, colder, and hence more dense layer beneath. Essentially all of the significant changes in these hydrographic properties occur in the upper layer which varies in depth from 5 meters to 15 meters throughout the estuary. Below 15 meters, temperature, salinity, and density exhibit only small changes, showing that this lower layer has homogeneous properties throughout.

Temperature varies from the highest values of 16°C at the surface to the generally consistent 8-9°C of the lower layer. The thermocline ranged in depth from 5-15m throughout the bay and over both days of the survey. The strength of the thermocline varied from .3 °C/m to 2 °C/m, but was usually on the order of 1 °C/m.

Salinity got as low as 25 PSU at the surface near the mouth of the river. The lower layer is consistently between 30-31 PSU throughout the bay. Density in the lower layer had a sigma-t value of 24, but the upper layer had sigma-t values as low as 18. Both the halocline and the pycnocline varied in depth from as shallow as 2m to depths closer to 10m. The pycnocline varied in strength from .2 units/m to .8 units/m, with an average of .6 units/m. The halocline averaged in strength at .5 PSU/m, varying by +- .3 PSU/m. The strength of both the pycnocline and halocline generally increased up the bay.

Preliminary calculations have shown that the density variations throughout Penobscot Bay are dominated by the salinity variations, not the temperature variations. Density is effected two to three times more by salinity than by temperature.

Some temporal variation of these hydrographic properties was observed in West Penobscot Bay over the two days of the hydrographic survey. The observations made on the first day were made during a flood tide and fairly high winds reaching 20 kn. The second day was essentially windless and the measurements were taken during an ebb tide. Temperature changes across similar transects were as follows. The surface temperatures increased from @16°C to @18°C. The lower level had a uniform temperature of 8°C during both days, but the 8°C isotherm progressed deeper by 5m or so. This downward progression of the thermocline was most likely due to vertical mixing caused by the heavy winds blowing on the surface layer during the first day.

Similarly, the halocline and pycnocline moved downwards presumably also due to this mixing. The surficial salinity values were slightly lower the second day peaking around 25 PSU as opposed to 26 PSU the day before. The range of density values was the same on both days, however, with sigma-t values of 18 at the surface to 24 for the lower layer.

Hydrographic spatial variations between East, West, and North Penobscot Bay, as well as within each bay were observed. Temperature variations were on the order of a few degrees and were mainly within the upper layer. Temperatures tended to be higher up estuary near the mouth of the river. Additionally, surface temperatures in the West Bay were consistently 2-3°C warmer than the East Bay counterparts. Salinity and density were constant in the lower layer, but generally decreased up the bay in the upper layer. Figures 1.25 and 1.26 show that there is stratification in the northern station profiles, but the other, more southern, station doesn't show much stratification at all, appearing to be fairly well mixed. This trend of more stratification nearer the river mouth and more uniform properties to the south was shown throughout the CTD data. It makes sense that the fresh water outflow from the river would cause greater stratification closer to the river mouth. Further south, the effect is lessened because the fresh water has more time and area to diffuse and mix with the saline Gulf of Maine water. See figure 1.27 for a density contour plot of a transect running north/south up the east bay. The isopycnals tend to outcrop towards the south, weakening the pycnocline.

Other Observations:

The Normandeau report (1975) gave a basic hydrographic picture which agrees with the above observations. They saw a two-layer system with an upper layer from 7-16m thick which showed seasonal variability, and a lower layer which was essentially isothermal and isohaline.

Hydrographic data for the transect from Turtle Head to Sears Island was collected in this report. It is difficult to compare these data sets because they were collected at different times of the year. The data set for this project was collected on July 5th and 6th, and the Normandeau (1975) data was collected on September 17th, 25th, October 16th, and December 11th. But one can hypothesize on the reasons for the observed differences.

The Normandeau temperature data shows a much smaller variation than the observed data and is significantly less stratified. By October 16th, there was no stratification, the whole water column being nearly 11°C. One possible explanation could be that as winter approached, there was less and less heating of the top layer by the sun, causing a decrease in strength of the thermocline and pycnocline. This would, by decreasing the vertical gradients, increase the possibility of vertical mixing of the

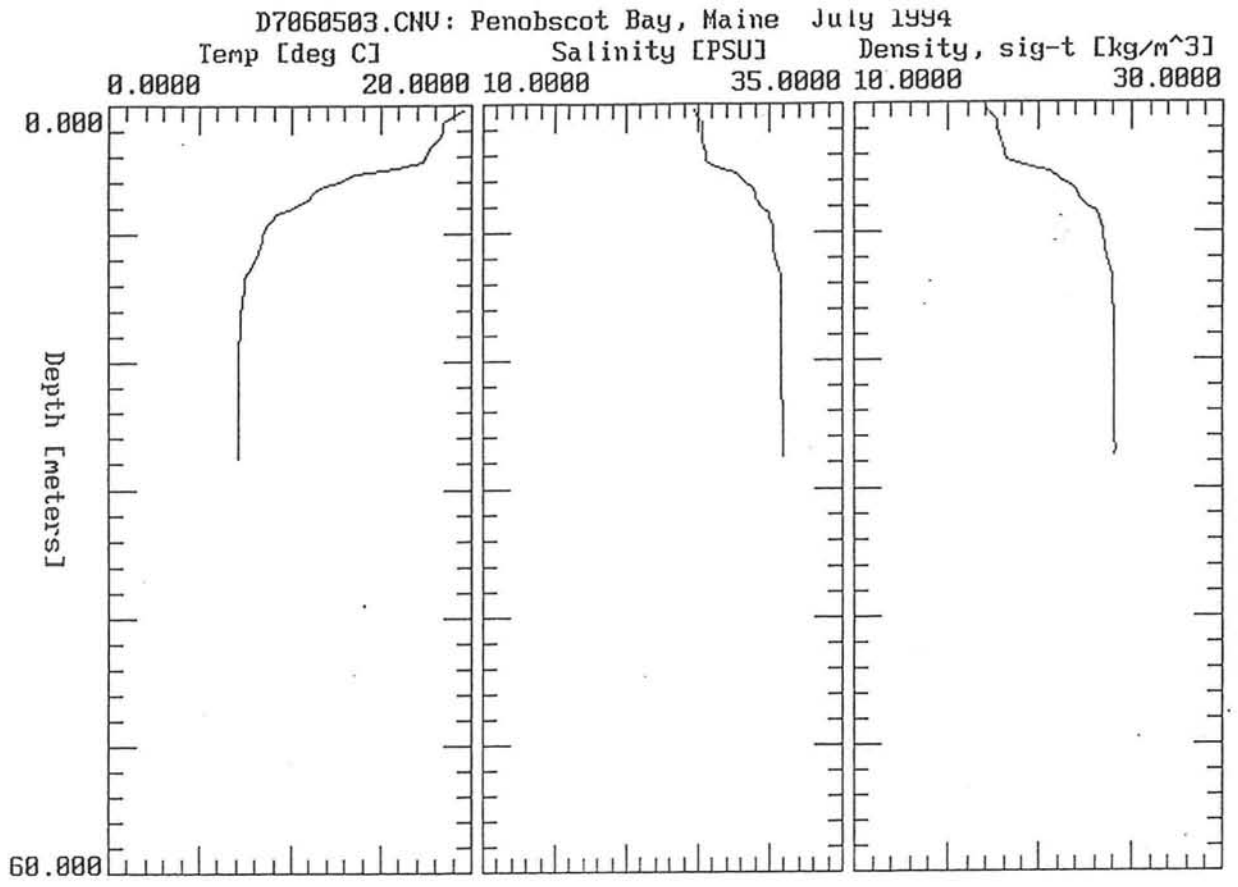

CTD Profiles - Northwest Penobscot Bay

Figure 1.25

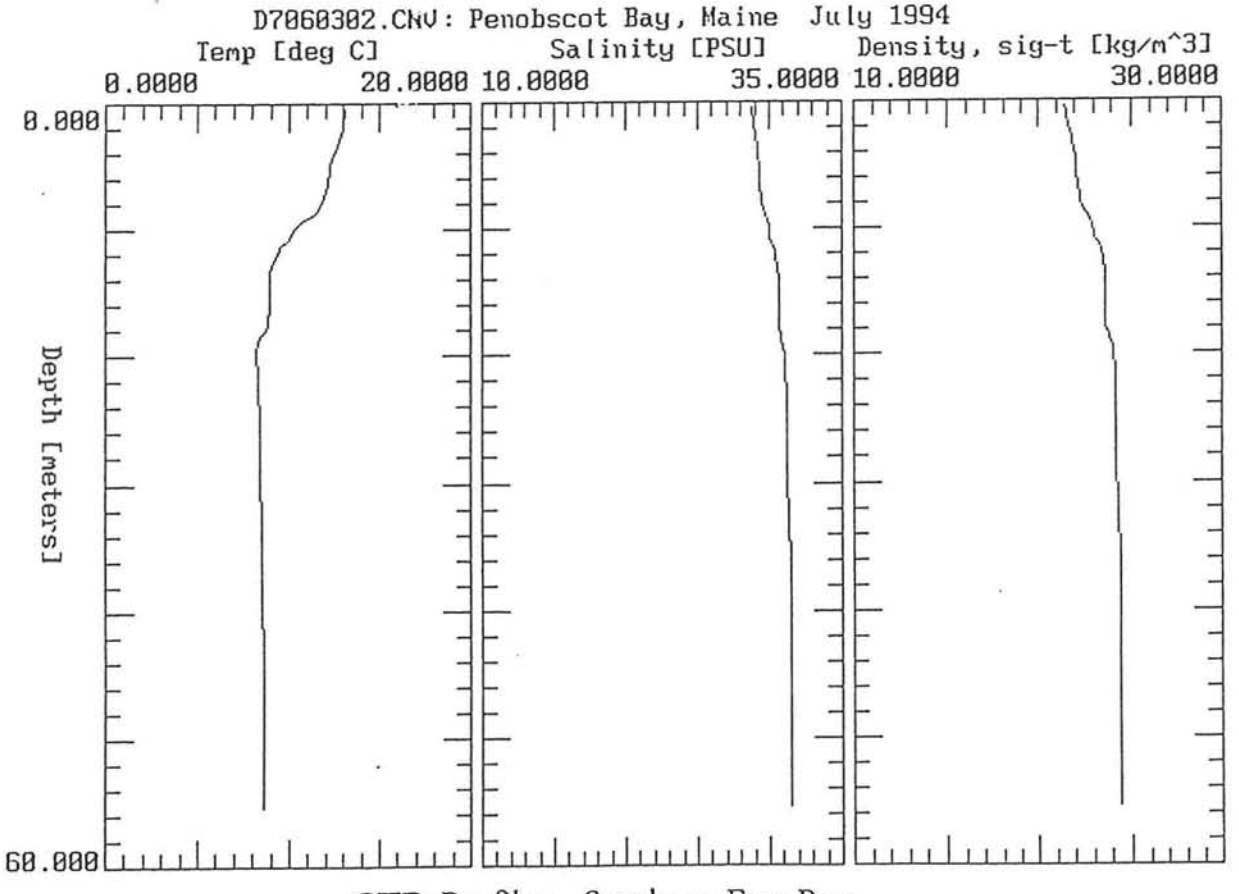

CTD Profiles - Southern East Bay

Figure 1.26

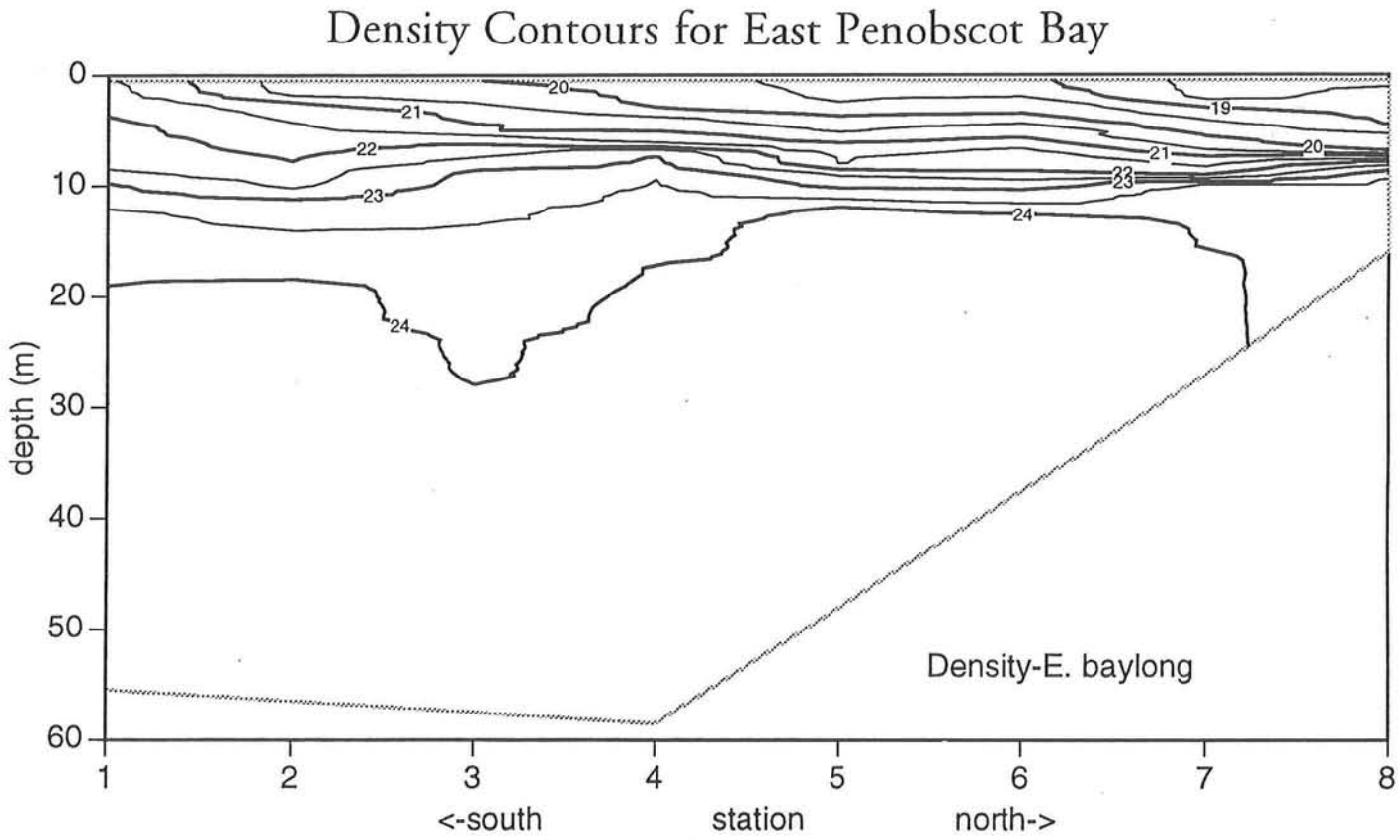
Density Contours for East Penobscot Bay
depth (m)
0
10
20
30
40
50
60
20
21
22
23
24
19
Density-E. baylong
1
2
3
4
5
6
7
8
<-south
station
north->

Figure 1.27

water column induced by storms or turbulence caused by tidal flow around local topography.

There were no significant variations of the salinity contours between the observed data and the Normandeau set. Density variations were small except the observed data showed lower surface densities by 2 units which could be accounted for by lower river outflow in the fall and early winter due to the retention of precipitation on land as a result of lower air temperatures.

Hydrographic data was collected by Haefner (1967) for the Penobscot River and the far northern reaches of the bay. The Haefner data set is larger and includes data taken at different times of the year. There is only a small region of overlap between Haefner's data set and the one collected for this paper, but they are in general agreement. There are no significant differences between what he observed and what has been discussed above.

Since Haefner collected data from different times of the year, he was able to discuss seasonal variations of the hydrography. There is generally less temperature stratification during the winter months, but as the sun begins to warm the upper layers as summer approaches, the water column gradually becomes stratified. Salinity varies in accordance with river outflow. In periods of high outflow, the salinity decreases more rapidly up the river, but in periods of low river outflow, the flooding tide is able to bring saline water further up the estuary.

Both vertical and horizontal mixing are important in the transport and spread of pollution. Since upper Penobscot Bay generally exhibits a moderate pycnocline, vertical mixing occurs mainly within the upper layer, above this pycnocline. Therefore waste discharged into the upper layer of the bay will tend to remain in this upper layer and be flushed out more quickly due to the general seaward motion of the upper layer. Horizontal mixing within this upper layer is significantly more important than vertical mixing because lateral diffusion tends to occur on isopycnals (Haefner, 1967).

Residence time calculations can provide valuable information on how long discharged pollutants will remain in the bay. Will they be flushed out quickly, or will they remain within the bay for an indefinite period of time? Residence time for the entire estuary was calculated using the simplified method found in Pickard and Emery, 1982. Pickard and Emery define residence time as

$$T_R = \frac{V}{V_i} \tag{1.3}$$

where V is the volume of the entire bay and V_i is rate of inflow into the bay. This essentially says that the residence time is the amount of time it would take to replace all of the water in the bay under given conditions. V_i is calculated in the following way.

$$V_i = \frac{X \cdot S_o}{S_i - S_o} \quad \text{where } X = (R+P) - E \tag{1.4}$$

S_o and S_i are the salinities of the water flowing out of and into the bay at the mouth of the bay. X is the amount of fresh water inflow which is calculated by river inflow plus precipitation $(R+P)$ minus evaporation (E). Values for each parameter were estimated from the literature and the observations. The residence time for material suspended in the upper layer was calculated by the above method to be close to 20 days.

OBSERVATIONAL CONCLUSIONS:

The hydrographic and current observations made in this study coupled with existing information yielded a fairly consistent first order picture of the physical characteristics of Penobscot Bay. Although no definitive overall circulation pattern was established, certain defining features of the flow were observed. The M2 tidal signal was not observed to be as dominant as thought. The currents appeared to include some sub-tidal components which are likely forced by wind stress and river outflow. The hydrography of the bay was determined to lie somewhere between moderately stratified and well-mixed depending on what time of year and the distance from the river mouth. The second section of this paper will use a numerical model in an attempt to define the elusive circulation in the bay. Both tidal and sub-tidal aspects of the current field will be investigated.

PART II: THE NUMERICAL MODEL

INTRODUCTION:

A numerical model for Penobscot Bay was developed in order to predict the tidal and sub-tidal currents as well as the sea surface displacements in the bay. The same basic model was used for the different types of currents, but the boundary conditions and forcing were modified. The study area for the model was enlarged from that of the field work so as to include all of Penobscot Bay rather than just the northern sections. The observations discussed in the first part of this report did not adequately describe the complex currents in the bay, but they did suggest that both tidal and sub-tidal currents are important in the overall circulation. Wind stress was suggested to be a major forcing of the currents, as was river outflow. The strength of the tidal currents and the geometry of the bay suggested that in addition to wind and river driven sub-tidal flows, there might exist sub-tidal flows generated by a tidally averaged vorticity flux (Zimmerman, 1981). This model was developed in an attempt to investigate the relative importance of tidal and sub-tidal currents.

FORMULATION:

The depth-averaged, shallow water representation of the equations of fluid motion in a rotating reference frame are used in the numerical model. In this model, density gradients as well as vertical structure of the flow are assumed to be negligible. This is not necessarily true for all locations in Penobscot Bay, as was shown in the first section of this paper, but in order to simplify the model, this assumption is made. This section develops and justifies the use of the aforementioned equations in Penobscot Bay.

The equations for conservation of momentum assuming hydrostatic balance in the vertical direction are as follows (Kundu, 1990; Csanady, 1982).

$$\frac{\partial u}{\partial t}+\overline{u}\cdot\nabla u = fv - g\frac{\partial h}{\partial x}+\frac{\partial}{\partial x}\left(A_H\frac{\partial u}{\partial x}\right)+\frac{\partial}{\partial y}\left(A_H\frac{\partial u}{\partial y}\right)+\frac{\partial}{\partial z}\left(A_V\frac{\partial u}{\partial z}\right) \quad (2.1)$$

$$\frac{\partial v}{\partial t}+\overline{u}\cdot\nabla v = -fu - g\frac{\partial h}{\partial y}+\frac{\partial}{\partial x}\left(A_H\frac{\partial v}{\partial x}\right)+\frac{\partial}{\partial y}\left(A_H\frac{\partial v}{\partial y}\right)+\frac{\partial}{\partial z}\left(A_V\frac{\partial v}{\partial z}\right) \quad (2.2)$$

Velocities are represented as $\overline{u}=(u,v,w)$; f is the Coriolis parameter which is assumed constant at 10^{-4} /s, g is the gravitational acceleration, 9.81 m/s^2, and A_H and A_V are the horizontal and vertical eddy viscosities respectively. Continuity for an incompressible fluid is given by:

$$\nabla\cdot\overline{u}=0 \quad (2.3)$$

All of the terms in the above momentum equations are not necessarily important in Penobscot Bay, so scaling arguments are used to simplify these equations. Typical scaling factors for Penobscot Bay are 1 m/s velocities, 10^5 m and 100m for horizontal and vertical length scales respectively, and 10^4 s as the time scale of one M2 tidal cycle. Typical values for A_H and A_V are 10^5 m^2/s and 10^{-2} m^2/s respectively (Kenefick, 1985). If these scaling factors are plugged into equations (2.1) and (2.2) certain terms are shown to be of much less importance than others. The non-linear terms as well as the term involving A_H are an order of magnitude smaller than the other terms so they will be neglected for the time being. The Rossby number, $(\mathrm{Ro}=U/fL)$, which is a non-dimensional measurement of the ratio of non-linear terms to the Coriolis term, is .1 for Penobscot Bay, further justifying the neglect of the non-linear terms in the model. The simplified equations of motion that are used in the model are:

$$\frac{\partial u}{\partial t} = fv - g\frac{\partial h}{\partial x}+\frac{\partial}{\partial z}\left(A_V\frac{\partial u}{\partial z}\right) \quad (2.4)$$

$$\frac{\partial v}{\partial t} = -fu - g\frac{\partial h}{\partial y}+\frac{\partial}{\partial z}\left(A_V\frac{\partial v}{\partial z}\right) \quad (2.5)$$

The continuity equation remains the same. If we integrate equations (2.4), (2.5) and continuity from the sea floor $(z=-H)$ to the sea surface $(z=h)$, we get

$$\frac{\partial U}{\partial t} - fV + g\frac{\partial h}{\partial x} + \left(Av\frac{\partial u}{\partial z}\right)_{z=-H} = 0 \tag{2.6}$$

$$\frac{\partial V}{\partial t} + fU + g\frac{\partial h}{\partial y} + \left(Av\frac{\partial v}{\partial z}\right)_{z=-H} = 0 \tag{2.7}$$

$$\frac{\partial}{\partial x}(UH) + \frac{\partial}{\partial y}(VH) + \frac{\partial h}{\partial t} = 0 \tag{2.8}$$

where U and V are the depth averaged velocities in the x and y directions respectively. The assumptions that h<<H and that there is no stress at the sea surface are made. The bottom friction terms are approximated with linear bottom friction of the form:

$$\left(Av\frac{\partial u}{\partial z}\right)_{z=-H} = \frac{r}{H}U \text{ and } \left(Av\frac{\partial v}{\partial z}\right)_{z=-H} = \frac{r}{H}V \tag{2.9}$$

r is the bottom drag coefficient for linear friction and is commonly given a value of 10^{-3} and has the units of m/s (Csanady, 1982) The final equations which form the basis of the numerical model are:

$$\frac{\partial U}{\partial t} - fV + g\frac{\partial h}{\partial x} + \frac{r}{H}U = 0 \tag{2.10}$$

$$\frac{\partial V}{\partial t} + fU + g\frac{\partial h}{\partial y} + \frac{r}{H}V = 0 \tag{2.11}$$

$$\frac{\partial}{\partial x}(UH) + \frac{\partial}{\partial y}(VH) + \frac{\partial h}{\partial t} = 0 \tag{2.12}$$

Finite-Difference Representation:

In order to solve this system of partial differential equations using a numerical model, the equations must be discretized. There are many different methods of finite-differencing a system of partial differential equations and each requires the use of a different discretization. In this model, the leap-frog time step is used in conjunction with centered spatial differencing. The equations were implemented on an A-grid, in which each variable (U,V,h) is calculated at every grid point. A representation of this grid is shown in figure 2.1. The subscripts i, j, represent the location of the grid point in x, y coordinates and the superscript n represents the time

step; n representing the current time step, n-1 the previous time step, and n+1 the next time step. The following are examples of how the partials were discretized.

$$\frac{\partial U}{\partial t} = \frac{U_{i,j}^{n+1} - U_{i,j}^{n-1}}{2\Delta t} \tag{2.13}$$

$$\frac{\partial h}{\partial y} = \frac{h_{i,j+1}^{n} - h_{i,j-1}^{n}}{2\Delta y} \tag{2.14}$$

This method of discretization was applied to the equations governing the system, yielding:

$$U_{i,j}^{n+1} = \frac{-g\Delta t}{\Delta x}\left(h_{i+1,j}^{n} - h_{i-1,j}^{n}\right) + 2\Delta t\left(fV_{i,j}^{n} - \frac{r}{H_{i,j}}U_{i,j}^{n-1}\right) + U_{i,j}^{n-1} \tag{2.15}$$

$$V_{i,j}^{n+1} = \frac{-g\Delta t}{\Delta x}\left(h_{i,j+1}^{n} - h_{i,j-1}^{n}\right) + 2\Delta t\left(-fU_{i,j}^{n} - \frac{r}{H_{i,j}}V_{i,j}^{n-1}\right) + V_{i,j}^{n-1} \tag{2.16}$$

$$h_{i,j}^{n+1} = \frac{-\Delta t}{\Delta x}\left(U_{i+1,j}^{n}H_{i+1,j} - U_{i-1,j}^{n}H_{i-1,j} + V_{i,j+1}^{n}H_{i,j+1} - V_{i,j-1}^{n}H_{i,j-1}\right) + h_{i,j}^{n-1} \tag{2.17}$$

Equations (2.15),(2.16), and (2.17) correspond to equations (2.10), (2.11), and (2.12) respectively. From these equations, the value of each variable at every grid point can be calculated for the n+1 time step from known values at time step n. The locations marked with X's in figure 2.1 show which values are used for the n+1 calculations. In discretizing the continuity equation, H was initially considered to be varying slowly enough that its spatial derivatives could be neglected. But in order to preserve some of the variations of H in the continuity equation, each neighboring velocity was referenced to the corresponding grid point's depth rather than to the central grid point depth (Kenefick, 1985). The frictional terms were calculated using velocities from the n-1 time step in order to maintain numerical stability (Kenefick, 1985). A square grid was used such that $\Delta x = \Delta y$.

One disadvantage of the A-grid used with centered differencing, as opposed to a C-grid, for example, (see Mesinger and Arakawa, 1976) is that neighboring grid cells are not linked to each other. In effect they are unable to communicate with each other. Hence, two sub-grids are created each of which are essentially independent of the other. This inadequacy often leads to a phenomenon called grid point oscillation in which high frequency waves with length scales on the order of the grid size are

A-Grid for finite-difference scheme

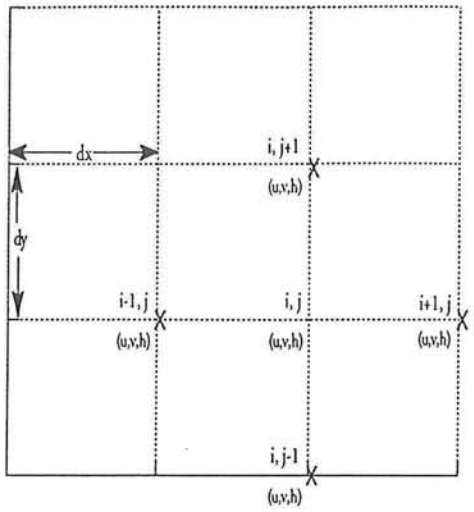

Figure 2.1

A-Grid - boundary calculation scheme

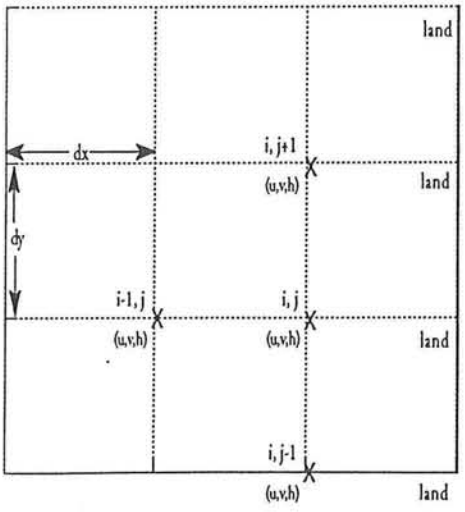

Figure 2.4

generated. In order to counter this grid point oscillation in the model, a smoothing function was introduced which performed a five point weighted average on every grid point every tenth time step. This effectively linked the two sub-grids and thereby eliminated the grid point oscillation.

The selection of appropriate grid dimensions and time step is essential to the accuracy of the model. For numerical stability, the model must be able to accurately represent gravity waves traveling from one grid point to the next. The maximum speed of shallow water gravity waves, which is directly related to the depth of the water in which they travel, therefore determines the relation between the spatial and temporal steps used in this finite difference approximation. The relationship is:

$$\Delta t < \frac{\Delta x}{\sqrt{g H_{\max}}} \tag{2.18}$$

This relationship is termed the CFL (Courant-Freidrich-Levy) stability criterion.

A square grid size of 800m was chosen for Penobscot Bay. This grid size was chosen so as to represent the general contour of the complex geometry without taking into account many of the smaller features. A smaller grid size would not only excessively complicate the geometry but would also increase the run time of the model without any significant increase in accuracy. A larger grid size wouldn't represent the geometry accurately and would likely overlook much of the spatial variability of the currents. The maximum depth of Penobscot Bay is approximately 120 m, and along with the grid size of 800 m, by equation 2.18, the time step must be smaller than 23 seconds. The time step was set at 10s to ensure numerical stability. The depth for each grid point was calculated from the on-line bathymetry data set available from U.S.G.S through Wood's Hole. This data set was parsed and gridded, yielding an average depth for each grid square. Unfortunately, the data set did not contain full coverage of the model study area, so in certain areas, the depths had to be estimated from values given on NOAA nautical chart #13302. The values pulled from the chart were rough estimates and therefore introduced some spiking into the data set. The spiking was removed by smoothing the data with a five point weighted average three times. $\partial H/\partial y$ was set to zero for a three grid points width swath at the open boundary. This was done in order to let the gravity waves, which were generated by the tidal height motion at the boundary, begin to propagate smoothly before encountering the complex topography. The grid representation of Penobscot Bay as

well as bathymetry contours are shown in figure 2.2. A mesh plot of the bathymetry is shown in figure 2.3.

Boundary Conditions and Forcing:

At the land/water boundaries, boundary conditions were specified and the finite-difference calculations were modified in order to account for the presence of the boundary. The no normal flow boundary condition was used such that velocities directed into land were set to zero. The south eastern edge of the study area is not bounded by land in a physical sense, but no flow through this boundary is specified in the model so as to limit the open boundary to only the southern edge. This boundary portion of the study area differs from a true land/sea boundary in that there is no shoaling of the bathymetry near it.

Due to the fact that for each calculation, velocity or height values at neighboring grid points are required, some modifications must be implemented at the boundaries. Non-centered differencing rather than centered differencing was used here. Since no values exist at land points, for each grid point touching a boundary, the value at the grid point was used for calculating the n+1 value instead of its neighboring land point. This decreases the distance between the points from which the gradient is estimated. This technique for calculating boundary values is shown in figure 2.4 and the corresponding, modified equations are shown below. Again, the X's mark which values are used to calculate the n+1 values. Non-centered differencing was also used at the open boundary for velocity calculations.

$$U_{i,j}^{n+1} = \frac{-2g\Delta t}{\Delta x}\left(h_{i,j}^{n} - h_{i-1,j}^{n}\right) + 2\Delta t\left(fV_{i,j}^{n} - \frac{r}{H_{i,j}}U_{i,j}^{n-1}\right) + U_{i,j}^{n-1} \qquad (2.19)$$

$$V_{i,j}^{n+1} = \frac{-g\Delta t}{\Delta x}\left(h_{i,j+1}^{n} - h_{i,j-1}^{n}\right) + 2\Delta t\left(-fU_{i,j}^{n} - \frac{r}{H_{i,j}}V_{i,j}^{n-1}\right) + V_{i,j}^{n-1} \qquad (2.20)$$

$$h_{i,j}^{n+1} = \frac{-2\Delta t}{\Delta x}\left(U_{i,j}^{n}H_{i,j} - U_{i-1,j}^{n}H_{i-1,j}\right) - \frac{\Delta t}{\Delta x}\left(V_{i,j+1}^{n}H_{i,j+1} - V_{i,j-1}^{n}H_{i,j-1}\right) + h_{i,j}^{n-1} \qquad (2.21)$$

In reality, no calculations for U would be made at this grid point due to the no normal flow boundary condition. The equation is written out here anyway to demonstrate the modifications that would have to be made to make the calculation. These equations

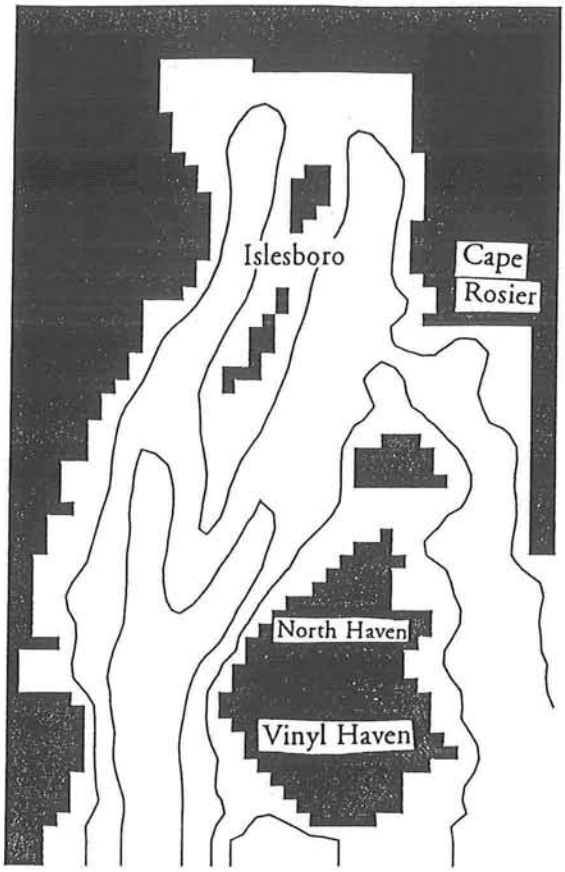

Grid and Bathymetry of Penobscot Bay

Depth Contours [20m, 50m]

Figure 2.2

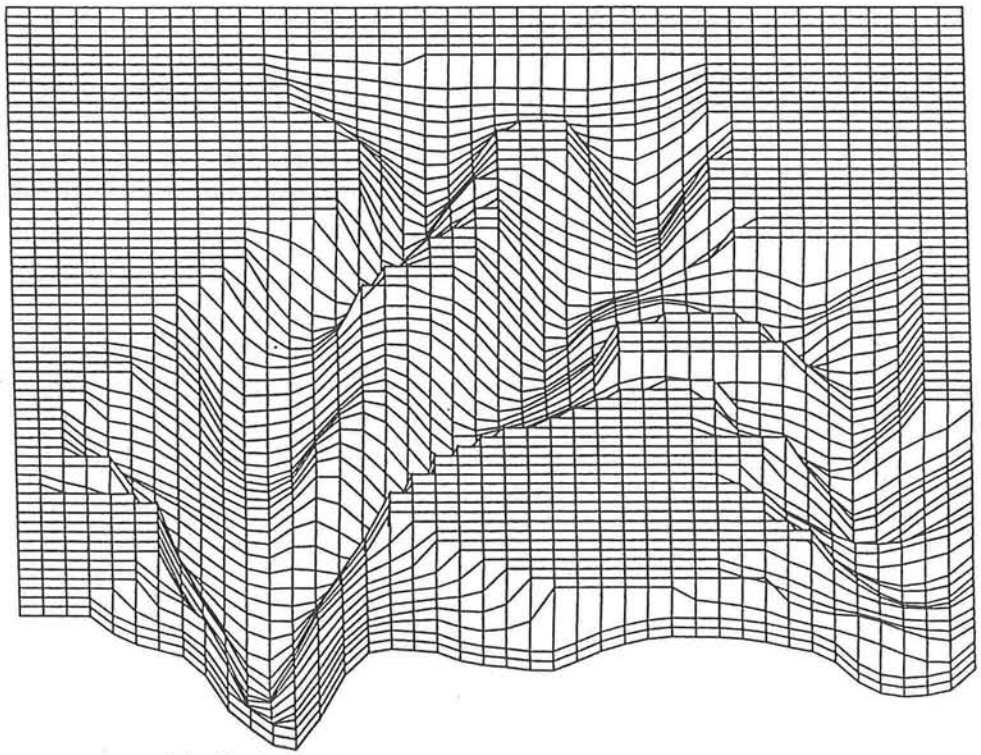

Mesh plot of Penobscot Bay bathymetry

Figure 2.3

can be modified accordingly for grid points with neighboring land points on different sides and for grid points with more than one neighboring land point.

The M2 tidal signal was introduced at the open boundary as the sole mode of forcing in the initial problem. The forcing was uniform across the mouth of the bay and was updated at the beginning of each time step. The forcing was a cosine wave specified by:

$$h_{i,j}^{n}\Big|_{\text{at open boundary}} = A\cos\left(\frac{2\pi}{T}t\right) \qquad (2.22)$$

A denotes the amplitude of the tidal wave which was set at 2m, and T is the period which was set to 12.4 hours; the period of the dominant M2 tidal component. The model was initialized with h, U, and V set to zero at every grid point. Then the time dependent forcing was introduced at the open boundary. The model ran for six tidal cycles before it reached an equilibrium periodic state in which the height values for similar stages of consecutive tidal cycles were equal. The model was run for ten tidal cycles to ensure that the equilibrium state was reached. The values of h, U, and V were recorded for every eighth of the final tidal cycle.

RESULTS:

Vector plots of velocity for each stage of the tidal cycle are shown in figures 2.5-2.12 and the sea surface displacement for the same stages is shown in figure 2.13. Velocities are shown to be on the order of 50 cm/s. The velocities are greater near the open boundary whereas the sea surface displacement is amplified near the head of the estuary as is common in estuaries. Although the flow here is solely tidal, the topography of the bay modifies the current patterns away from the simple in and out tidal flows that are seen in geometrically simpler embayments. For example, at high tide, a clockwise circulation around Islesboro Island exists. This circulation switches direction at low tide. At mid-flood or mid-ebb, the velocities are stronger and are directed in and out of the bay, flowing around the islands. The Coriolis force appears to play a minor role in the tidal solution, as there exist only very slight lateral sea surface height differences in the bay.

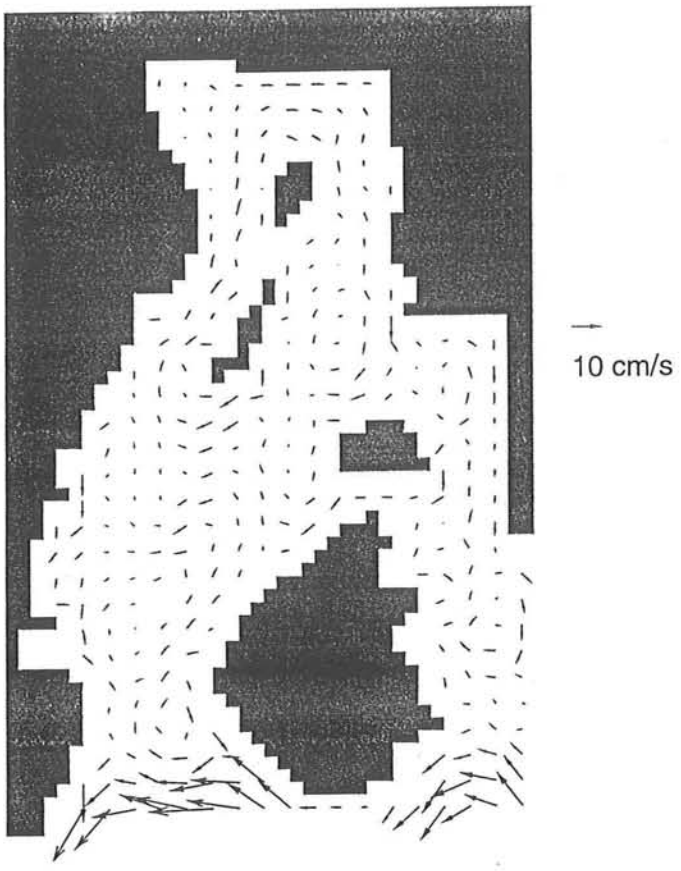

stage = 0 (high tide)

Figure 2.5

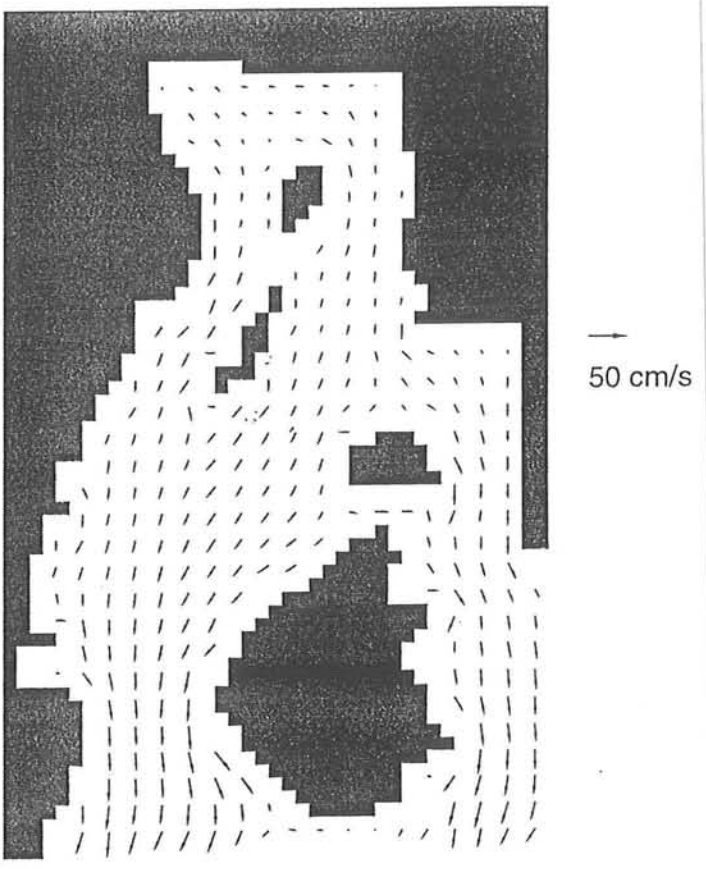

stage = 1

Figure 2.6

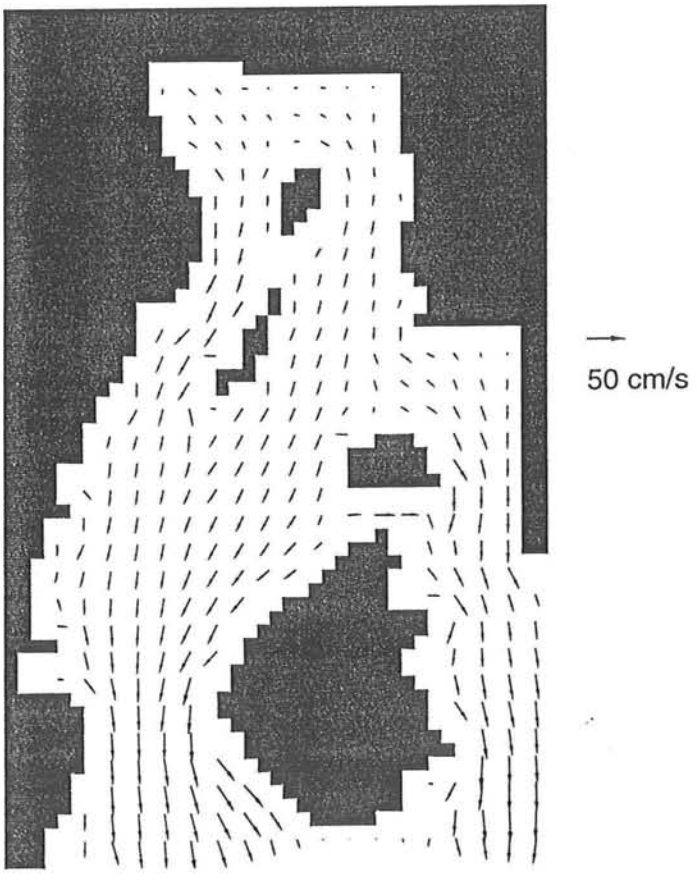

stage = 2 (mid–ebb)

Figure 2.7

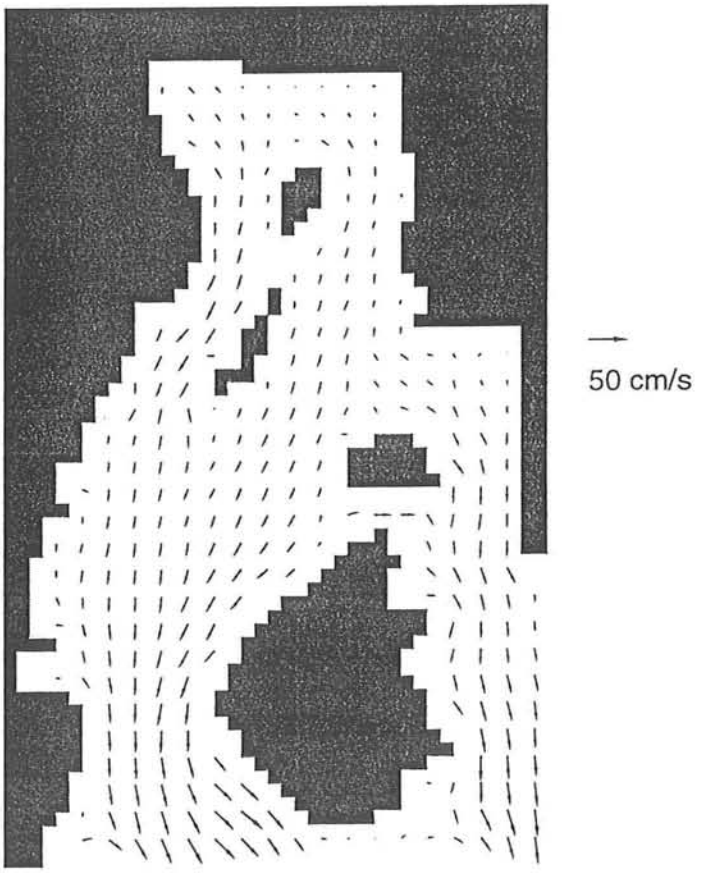

stage = 3

Figure 2.8

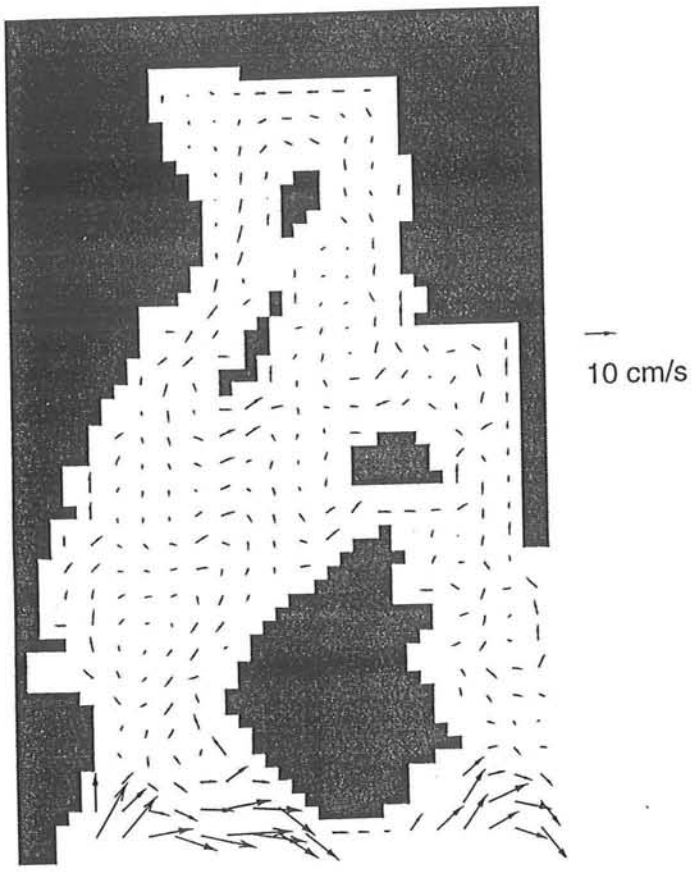

stage = 4 (low tide)

Figure 2.9

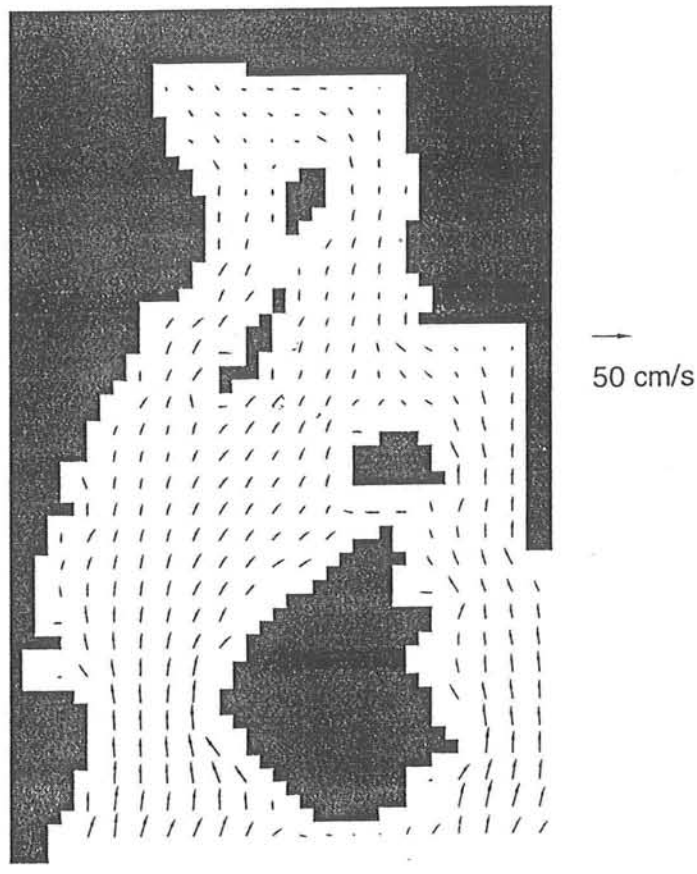

stage = 5

Figure 2.10

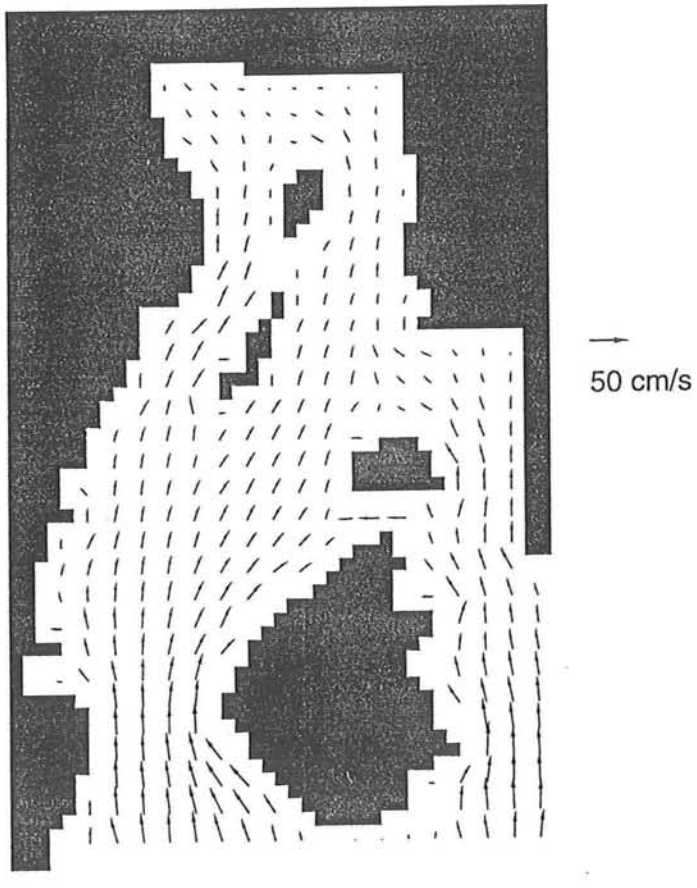

stage = 6 (mid–flood)

Figure 2.11

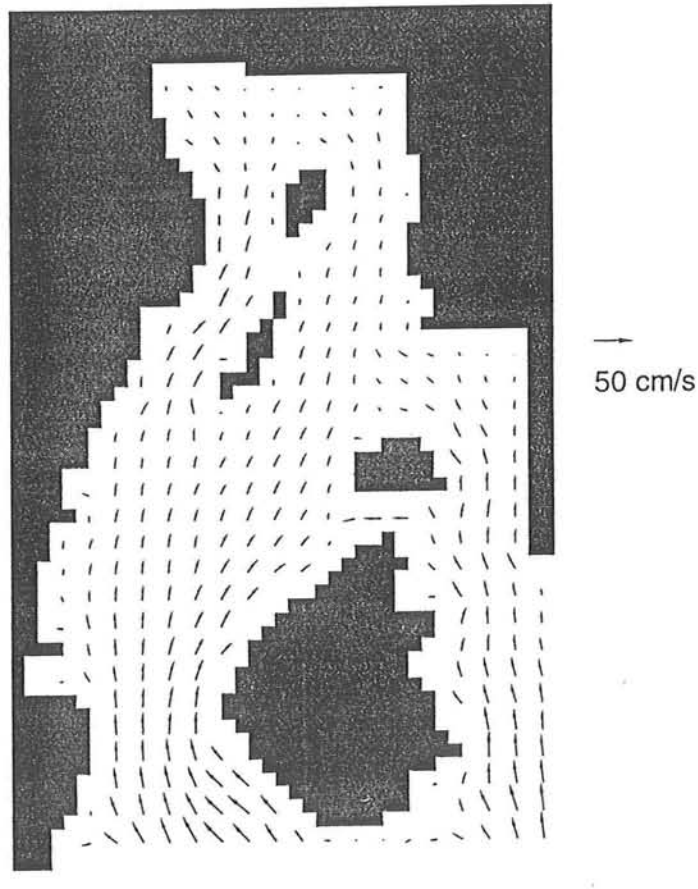

stage = 7

Figure 2.12

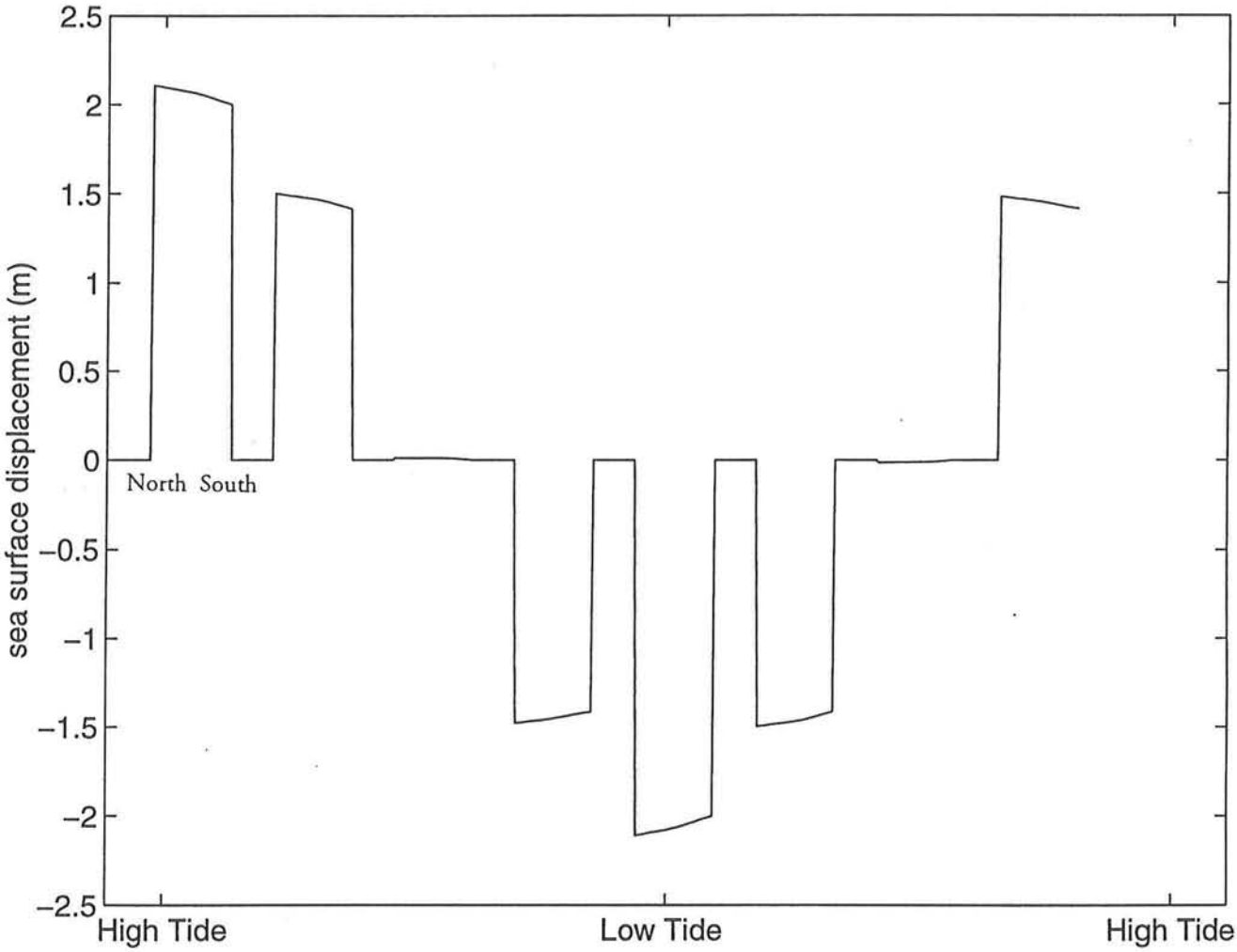
2.5
2
1.5
1
0.5
0
−0.5
−1
−1.5
−2
−2.5
sea surface displacement (m)
North South
High Tide
Low Tide
High Tide

Figure 2.13

Comparison of Model To Observations:

It is standard for numerical models to be tested by some comparison of the predicted values to observed values. These types of comparisons can quantify the accuracy of a model. For example, Kenefick (1985) compared his model results for Long Island Sound to observed tidal heights at various locations within the sound. Unfortunately comparisons of this type cannot be made for this numerical model because the observations are far too sparse for any conclusive results to be obtained. This model was designed to give an accurate first order picture of the tidal circulation. Therefore certain simplifications were made such as spatially independent forcing at the open boundary with an estimated amplitude. In order to be entirely accurate, the model should have been forced with actual tidal height data from stations along this boundary with the interior heights determined from a linear interpolation (Taylor, 1919; Kenefick, 1985). Certainly this modification would create small differences in the values for velocity and sea surface displacement, but the first order picture would likely remain unchanged. Also, the linear parameterization of friction used in the model does not necessarily accurately represent the frictional damping that actually occurs in the bay. Due to these simplifications, a direct, numerical comparison of model to observations would not be useful as the first order picture is the main concern.

The model's accuracy was shown by its general agreement with the literature and what was shown from the observations. Both this model and the simple three parameter model used to fit the observational data showed a tidal velocity amplitude of around 20 cm/s in the upper portions of the bay. The amplitude of the tidal height, as mentioned before, increased towards the head of the bay which agrees in trend and in magnitude with the data given in Normandeau (1975) for different stations in the bay.

SUB-TIDAL CURRENTS:

The tides in Penobscot Bay are the dominant forcing behind the currents. But by their nature, they are periodic and are therefore relegated to a secondary role in the transport of pollution and other suspended materials. Sub-tidal currents play a much more important role in this area and can define the overall circulation pattern of an estuary despite their smaller magnitude. There are many different forcing mechanisms that can drive such circulation. The above numerical model will be

extended to investigate three such forcing mechanisms; tidally averaged vorticity flux, wind stress, and river outflow.

Tidally Averaged Vorticity Flux:

Although tidal currents are periodic, they can generate residual, time-independent currents of a smaller magnitude by the net transfer of vorticity from the tidally oscillating field to the mean field (Zimmerman, 1981). This transfer of vorticity arises from variations in the topography and morphology which in turn give rise to spatial variations in the frictional drag. Zimmerman discusses three idealized morphological situations which provide favorable conditions for this vorticity transfer. These are residual basin circulation, headland eddies, and sand ridge eddies. Only the first will be discussed as it pertains closest to Penobscot Bay. Residual basin circulation occurs in semi-enclosed basins usually with one boundary open to the sea where the tidal forcing is introduced (see figure 2.14). The tidal velocities are maximum in the center of the bay, where there is no frictional effect from the boundaries, and diminishes to zero at the side walls and the head of the basin. As the tide comes in, velocities are in the direction of the solid arrows. Near the boundaries, there is horizontal shear in the flow because the velocities decrease towards the boundaries. At the upper boundary, this shear creates negative vorticity shown by the solid circles drawn in the diagram. The currents are moving into the bay here, so the net result is a transfer of negative vorticity into the bay. In the ebb tide, the velocities reverse direction, and by the same argument, positive vorticity is generated (dashed circle). Therefore in the ebb tide, there is a net transfer of positive vorticity out of the bay, which is the same as a net transfer of negative vorticity into the bay. In this fashion, vorticity is built up in certain regions within the bay until it reaches a steady state balanced by frictional dissipation.

In order to quantify this vorticity transfer, Zimmerman uses the concept of circulation to show how vorticity is related to residual eddies in a tidally oscillating field. The following formulation is paraphrased from Zimmerman. Figure 2.15 is taken from Zimmerman and shows a time independent vortex in an oscillating tidal field where the instantaneous velocity vector is defined as

$$\overline{u}(t) = \overline{u}_{\parallel}(t) + \overline{u}_{\perp}(t) \qquad (2.23)$$

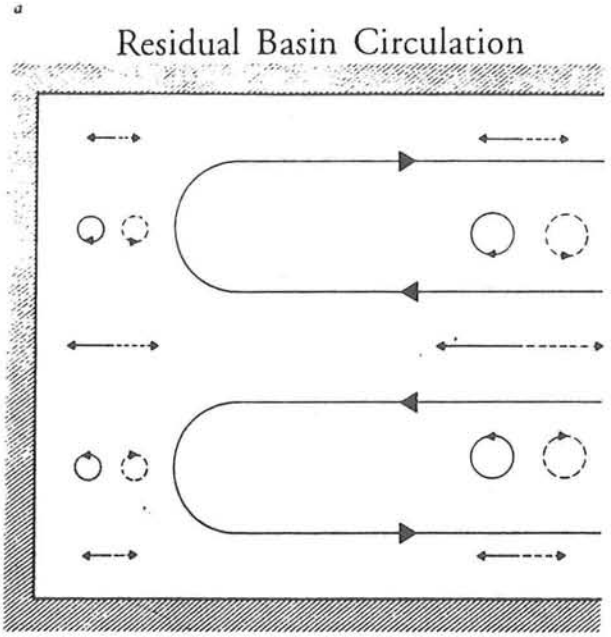

Figure 2.14

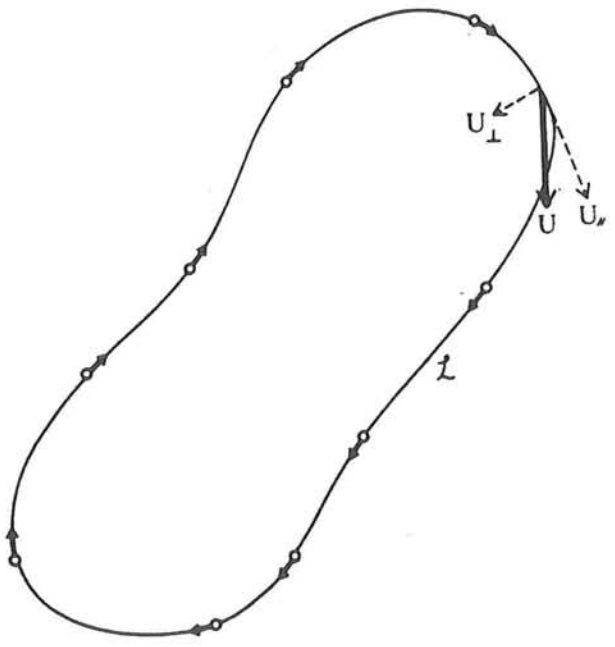

Figure 2.15

where $\overline{u}(t) = (u(t), v(t))$. Taking the tidal averages of the velocity vectors (denoted by<>) we find that

$$\langle \overline{u}_{\perp} \rangle = 0, \quad \langle \overline{u}_{\parallel} \rangle = \overline{u} \tag{2.24}$$
$$\overline{u}_{\perp} = A\sin(\sigma t + \phi_{\perp}), \quad \overline{u}_{\parallel} = \langle \overline{u}_{\parallel} \rangle + B\sin(\sigma t + \phi_{\parallel})$$

A and B are constant amplitudes and $\phi_{\perp}$ and $\phi_{\parallel}$ are arbitrary phase angles. The only time independent component of velocity is in the $\overline{u}_{\parallel}$ direction. Circulation can be defined as the contour integral of velocity,

$$C = \oint \overline{u} \cdot \mathrm{d}l = \oint u_{\parallel}(t) dl \tag{2.25}$$

By Stokes theorem and the definition of vorticity, ω, this becomes an area integral of vorticity.

$$C = \iint_A \omega dA \text{ where } \omega = \nabla \text{ x } \overline{u} \tag{2.26}$$

By averaging this equation over a tidal cycle, it can be seen that in order for a tidally averaged residual circulation to exist, there must be a tidally averaged build-up of vorticity (positive or negative) for the particles enclosed in the area.

$$\langle C \rangle = \oint \langle u_{\parallel} \rangle (t) dl = \iint_A \langle \omega \rangle dA \tag{2.27}$$

Vorticity appears in the momentum equation only as a non-linear term. In the tidal model, these non-linear terms were thrown out in the scaling analysis, assuming that they were unimportant in the tidal solution. But now that we are concerned with the residual currents not the tidal currents, the non-linear terms must be considered. Zimmerman uses the following form of the momentum equation for "quasi two-dimensional homogeneous fluid flow in a rotating frame of reference":

$$\frac{\partial \overline{u}}{\partial t} = -\{f + \omega\}\left(\hat{j} \text{ x } \overline{u}\right) + \nabla\left(gh + \frac{u^2}{2}\right) - \frac{r}{H}\overline{u} + \nu\nabla^2\overline{u} \tag{2.28}$$

The last term, which represents the horizontal turbulent momentum exchange, is neglected. Taking the derivative of (2.25) with respect to time and substituting for $\partial\bar{u}/\partial t$ from (2.28) we get,

$$\frac{\partial C}{\partial t} = \oint \{f + \omega\} u_{\perp} dl - \frac{r}{H} C \tag{2.29}$$

where $\hat{n}$ is the direction perpendicular to the contour around which the integral is taken. The pressure gradient term disappears because the contour integral of a gradient is zero. If we now average this equation over a tidal cycle both $\langle \partial C/\partial t \rangle$ and $\langle fu\ dl \rangle$ equal zero, leaving:

$$\langle C \rangle = \frac{\oint \langle \omega u_{\perp} \rangle dl}{r/H} \tag{2.30}$$

The term inside the contour integral is the spatially-varying, tidally-averaged vorticity flux and can be calculated for each grid point in the tidal model. Wherever this term is non-zero, a "tidal stress" is created which leads to a time independent circulation.

Vorticity was calculated by the following discretization in the model.

$$\omega^n_{i,j} = \frac{V^n_{i+1,j} - V^n_{i-1,j} - U^n_{i,j+1} + U^n_{i,j-1}}{2\Delta x} \tag{2.31}$$

At the boundaries, the velocities of land points were set to zero. For each grid point, the product of vorticity and velocity was added up over an entire tidal cycle and divided by the number of time steps in a tidal cycle. This process yielded two "forcing arrays", one of $\langle \omega U \rangle$ for each grid point and one of $\langle \omega V \rangle$ for each grid point. Figures 2.16 and 2.17 show how this vorticity flux varies spatially within the bay. The magnitudes are greater near the land/sea boundaries where shoaling exists as expected. These forcing arrays were then used to drive the numerical model instead of driving it with varying sea surface displacement at the open boundary. The model will now simulate the residual currents driven by vorticity flux. The continuity equation remains the same, but the momentum equations become:

$$\frac{\partial U}{\partial t} - fV + g\frac{\partial h}{\partial x} + \frac{r}{H} U = \langle \omega V \rangle \tag{2.32}$$

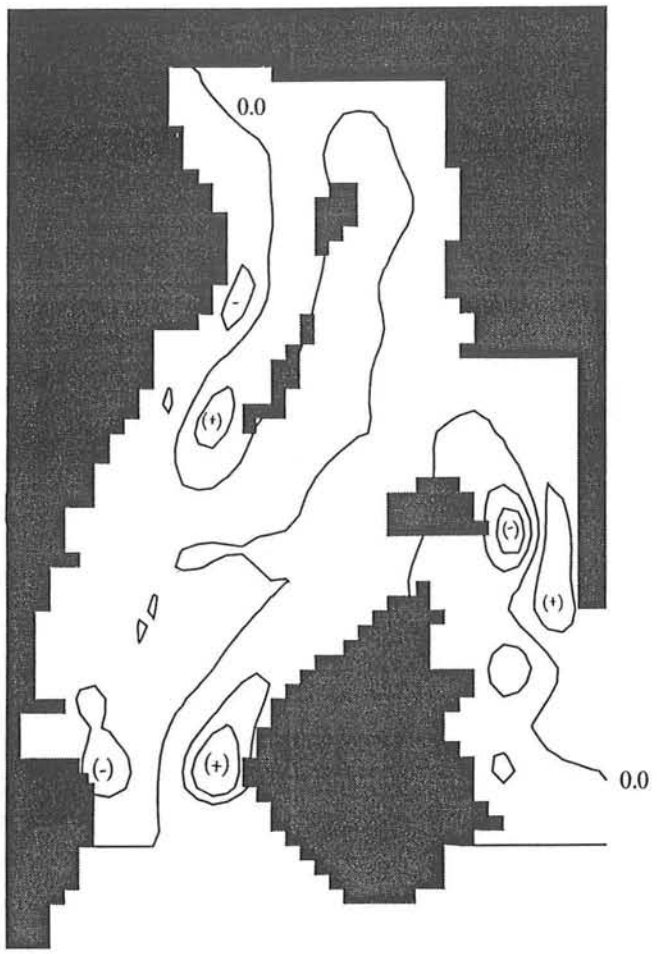

Tidally Averaged Vorticity Flux <ωv>

Contour values [$-1x10^{-5}$, $-5x10^{-6}$, 0.0, $5x10^{-6}$, $1x10^{-5}$] (m/s^2)

Figure 2.16

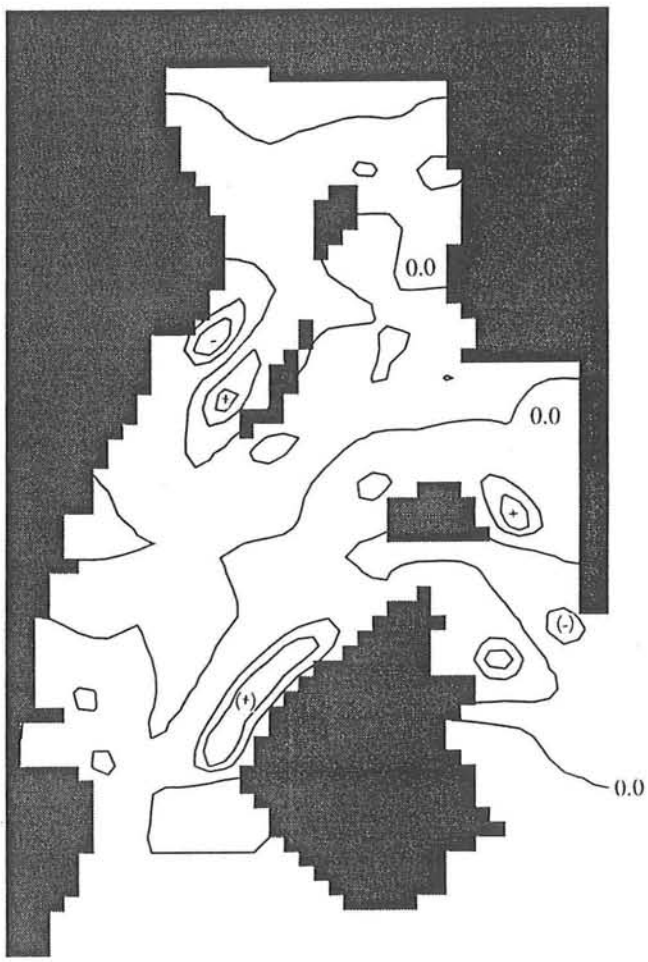

Tidally Averaged Vorticity Flux <ωu>

Contour values [$-3x10^{-6}$, $-2x10^{-6}$, 0.0, $2x10^{-6}$, $3x10^{-6}$] (m/s^2)

Figure 2.17

$$\frac{\partial V}{\partial t} + fU + g\frac{\partial h}{\partial y} + \frac{r}{H}V = -\langle \omega U \rangle \tag{2.33}$$

The right hand terms are the vorticity flux forcing terms which drive the model. These equations are discretized in the code as:

$$U_{i,j}^{n+1} = \frac{-g\Delta t}{\Delta x}\left(h_{i+1,j}^{n} - h_{i-1,j}^{n}\right) + 2\Delta t\left(fV_{i,j}^{n} - \frac{r}{H_{i,j}}U_{i,j}^{n-1} + \langle \omega V \rangle_{i,j}\right) + U_{i,j}^{n-1} \tag{2.34}$$

$$V_{i,j}^{n+1} = \frac{-g\Delta t}{\Delta x}\left(h_{i,j+1}^{n} - h_{i,j-1}^{n}\right) + 2\Delta t\left(-fU_{i,j}^{n} - \frac{r}{H_{i,j}}V_{i,j}^{n-1} - \langle \omega U \rangle_{i,j}\right) + V_{i,j}^{n-1} \tag{2.35}$$

The model was run until it reached a steady state in which the vorticity flux is balanced by frictional damping. At the open boundary, the gravity wave radiation boundary condition was used which allows for outwardly traveling gravity waves to continue to travel out of the model region without being reflected. This boundary condition can be stated as:

$$h\big|_{\text{at open boundary}} = \sqrt{H/g}\left(\overline{U} \cdot \hat{n}\right) \tag{2.36}$$

where $\hat{n}$ is the vector normal to the open boundary (Bogden, personal correspondence).

The tidally induced residual current field is shown in figure 2.18. The currents are one to two orders of magnitude smaller than the tidal currents. The current field is not as nicely defined as the tidal signal, but there are several notable features. Three areas of larger residual currents are created. The larger currents occur near the boundaries because this is where there exists horizontal shear due to the sloping up of the bottom towards land. There is no horizontal friction in this model, so it must be simulated by bottom friction. The parameterization of friction used in the model therefore becomes an important factor in defining this residual circulation. To accentuate the frictional effects the model was run with a modified bathymetry file that uniformly increased the shoaling at all land/sea boundaries. The results of this are shown in figure 2.19. One can see that this effective boost of the frictional term at the boundaries has a moderate effect on the residual currents by increasing their strength. The general flow field is similar, though.

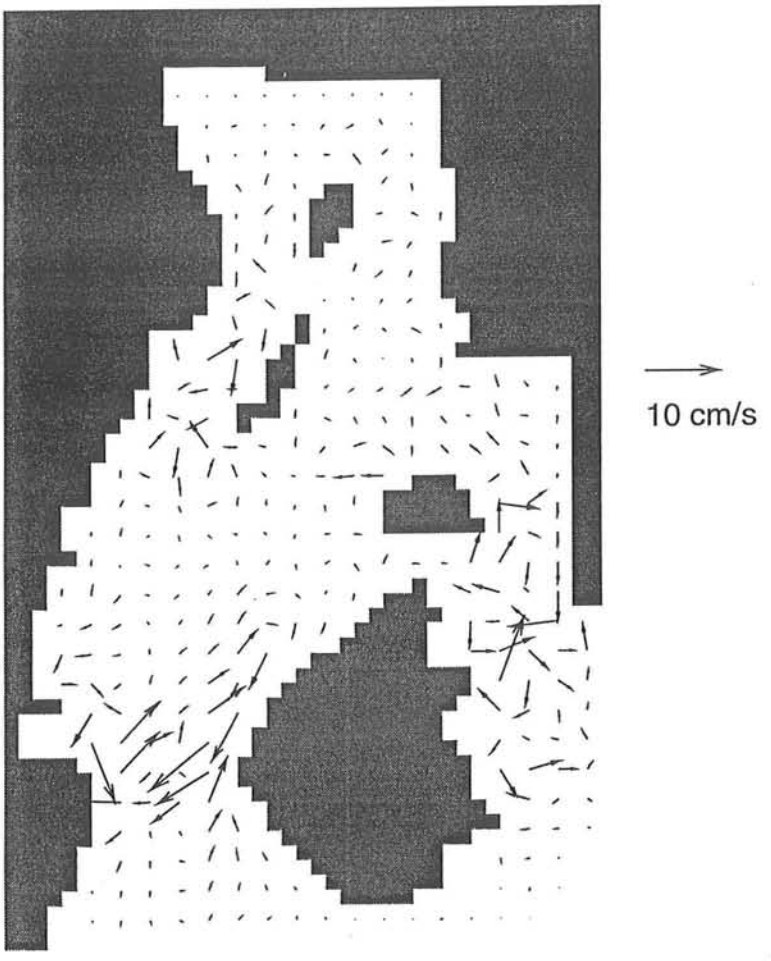

Tidally induced residual currents

Figure 2.18

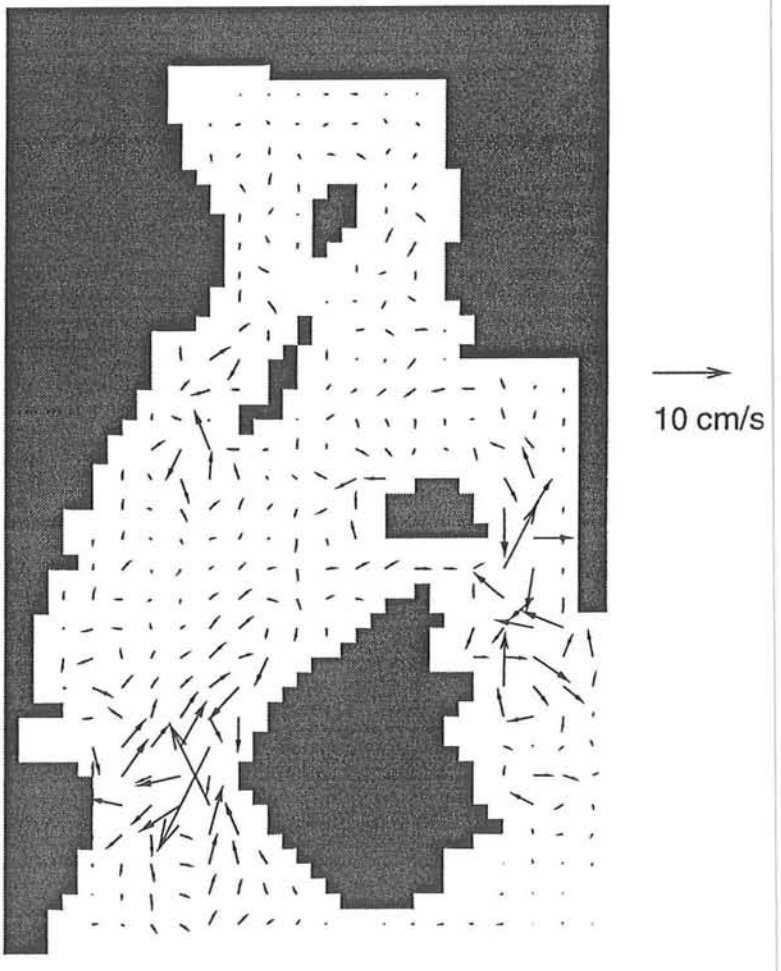

Tidally induced residual currents with modified bathymetr

Figure 2.19

The topography of Penobscot Bay is considerably more complex than that of the idealized residual basin circulation discussed above, so the idealized circulation is not seen. In certain areas, however, one can see that the currents are directed out of the bay near the boundary and into the bay away from the boundary. The vortex just west of North Haven exhibits this feature as does the circulation pattern to the west of Islesboro. Also from figure 2.16, one can see from the zero contour line that the two channels in the upper bay are neatly divided down the center into areas of positive and negative vorticity flux. This is in accordance with Zimmerman's residual basin circulation.

The order of magnitude of the forcing terms was between 10^{-5} and 10^{-6} m/s^2. The forcing varied spatially throughout the bay and therefore tended to drive only local currents, not some overall circulation pattern. The basic dynamical balance set up in these local areas of stronger residual currents was a balance between the forcing term and the frictional term.

$$\frac{r}{H}U = \langle \omega V \rangle \text{ and } \frac{r}{H}V = -\langle \omega U \rangle \tag{2.37}$$

In the shallower areas, the frictional damping is greater. The forcing term tends to be larger near shore also, as discussed above. At the steady state, the other terms in the momentum equation play a minor role.

Wind Stress:

Wind blowing over the surface of the water can induce fluid motion in the underlying water by means of a vertical propagation of horizontal shear. Through this mechanism, currents of the same direction as the wind are generated in the fluid. The wind will affect the surface layer of fluid more than the underlying layers, but since this model is two-dimensional, this cannot be directly simulated. The wind forcing is introduced into the model as an inverse function of H, (τ/H), creating a larger wind driven current in the shallower areas. $\overline{\tau}$ is the wind stress, which is a function of wind speed. The equations of motion become:

$$\frac{\partial U}{\partial t} - fV + g\frac{\partial h}{\partial x} + \frac{r}{H}U = \frac{\tau_x}{H} \tag{2.38}$$

$$\frac{\partial V}{\partial t} + fU + g\frac{\partial h}{\partial y} + \frac{r}{H}V = \frac{\tau_y}{H} \qquad (2.39)$$

All other forcing mechanisms have been removed so as to examine only the wind driven currents. $\overline{\tau}$ was given a value of .0001 m^2/s^2 which corresponds to a 14 knot wind. The magnitude of this forcing term is the same as that of the vorticity flux forcing term. Winds of this magnitude are prevalent in Penobscot Bay during the summer. Winds in the summer are generally from the south, although they vary from southeast to southwest (Normandeau, 1978). With this in mind, the model was run three times with uniform wind stresses from the south, southeast, and southwest. The gravity-wave radiation boundary condition was used at the open boundary again. Once the system reached a steady state, the velocity and sea surface displacement were recorded. These are shown in figures 2.20-2.22 for each of the three wind directions. The spin-up time for the wind driven currents was on the order of one day. The wind driven currents are moderately affected by changes of wind direction of 45 degrees.

The general flow pattern was for the currents to be in the same direction as the wind stress in shallower areas and to be directed oppositely in the deeper areas. This was expected because the wind stress was applied as a function of water depth which causes a greater stress to be applied to the shallower areas. The water that is pushed up estuary by the wind must return south somehow and it does this where the wind stress is weakest; in the deep, mid-channel areas. This pattern is most apparent when the wind is blowing directly from the south. A fairly well-defined clockwise circulation around Islesboro was generated by the southwesterly breeze. This circulation was vaguely shown throughout the literature, as discussed in section 1. Wind stress was introduced as a uniform stress with no spatial variations as opposed to the spatially varying stress introduced by vorticity flux. Therefore, it is expected that the nature of the currents generated will be different. The wind generated an overall circulation pattern with only small variations in magnitude throughout the bay, as opposed to the localized areas of strong current and weak current generated by the vorticity flux forcing.

The basic dynamical balance that is set up and maintained when the steady state is reached is a balance between the wind stress term and the forcing term. The other terms are of lesser importance in the steady state. This balance is mathematically stated as the following simplification of the momentum equations used in the model.

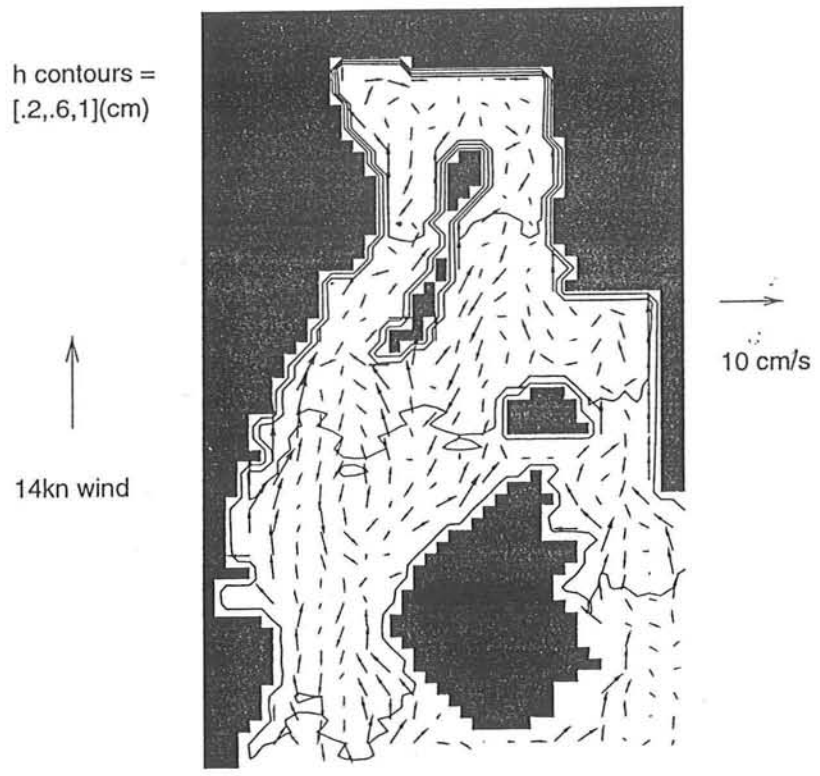

Steady-state currents from S wind

Figure 2.20

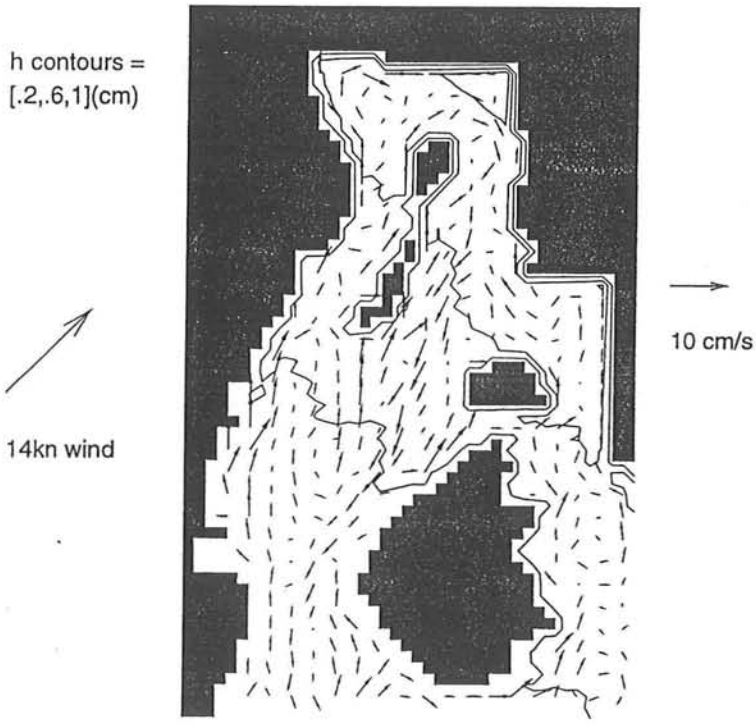

Steady-state currents from SW wind

Figure 2.22

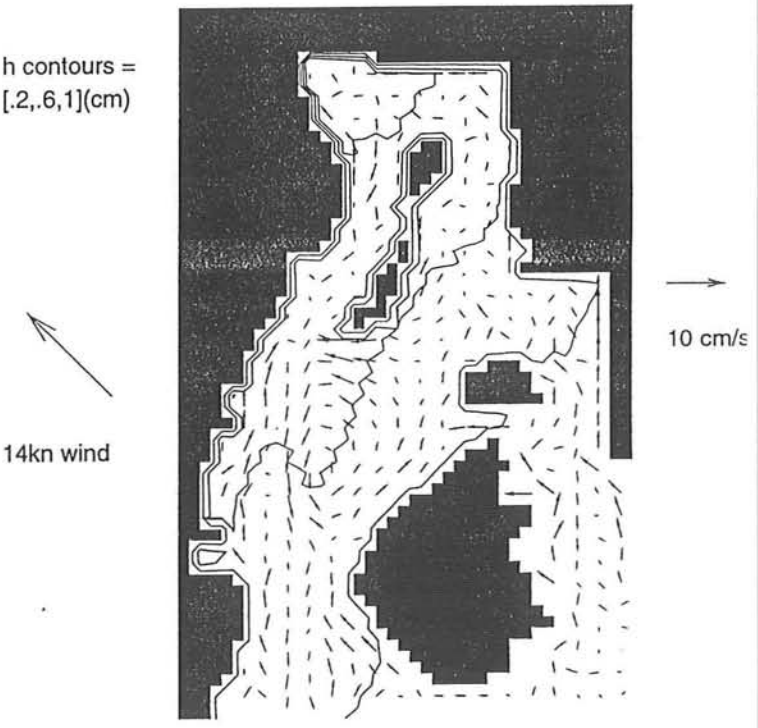

Steady-state currents from SE wind

Figure 2.21

$$\frac{\tau_x}{H} = g\frac{\partial h}{\partial x} \quad \text{and} \quad \frac{\tau_y}{H} = g\frac{\partial h}{\partial y} \tag{2.40}$$

This balance is the overall balance, but local currents occur and are governed by different balances. Near the shore, the frictional damping is greater due to the smaller depth. In these areas, a balance between frictional damping and the wind stress is set up. The pressure gradient mentioned above plays a secondary role here, but in the deeper areas where the wind stress is lessened, the pressure gradient becomes more dominant in the dynamical balance. In these locations, the wind stress plays the minor role and the dominant balance is between the pressure gradient and friction.

River Outflow:

The Penobscot River does produce a large outflow of fresh water into the estuary. This fresh water flows out at the mouth of the river in the surface layer because it is lighter than the salty bay water. This outflow sets up density gradients in the vertical which can lead to thermohaline circulation. Unfortunately, this model is limited to two-dimensional flow, so the effects of river outflow on the currents in the bay cannot be fully investigated with this model. Despite these limitations, the model was adapted to simulate the depth averaged currents which would arise from river outflow in the northeastern corner of the bay. The average river outflow was estimated from data available from U.S.G.S and Normandeau (1978). A depth averaged flow was determined for a six grid point wide river mouth. This flow was introduced as a boundary condition in which the v velocity was specified at these boundary points. The outflow was given a rough cosine shape with velocities stronger near the central grid points and trailing off towards the edges so as not to introduce unnatural horizontal shear into the flow. The velocities were specified over several grid points width in the y-direction in order to link the neighboring grid points in an attempt to lessen any grid point oscillation that might occur.

The model was run until it reached a steady state with no forcing other than this boundary condition. The equations were the same as for the tidal model (see eqns (2.10), (2.11), and (2.12) with discretizations (2.15), (2.16), and (2.17) respectively). The open boundary sea surface displacement values were calculated using the gravity wave radiation condition. The results of this model run are shown in figure 2.23. One can see that not very much information about the river driven current field can be obtained from this model run. The currents simply move southward around the

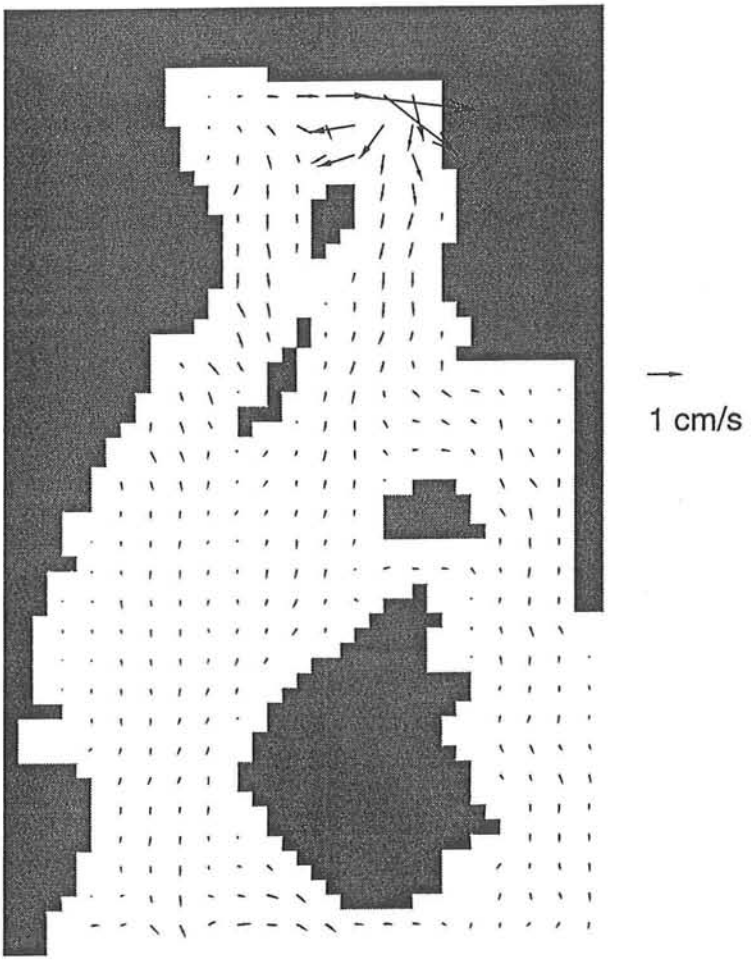

Figure 2.23

topography from the mouth of the river to the mouth of the bay. The currents are strongest near the river mouth and decrease southwards as would be expected. In this case, the forcing is local, generating only locally strong currents. The dynamical balance set up by this forcing is between the pressure gradient and friction. The result of this balance is the down gradient flow seen. Due to the inadequacies of this model in predicting the effects of river outflow, it is difficult to gauge, from the model output, the importance of river outflow on the currents in Penobscot Bay.

CONCLUSIONS:

The numerical model has not only been used to investigate the response of Penobscot Bay to tidal forcing, but in addition to look at three other forcing mechanisms which can give rise to a sub-tidal circulation. The tidal components are shown to be one order of magnitude greater than the sub-tidal currents. Both tidally induced vorticity flux and wind stress are shown to drive significant sub-tidal currents on the order of 5 cm/s. This magnitude is in agreement with Humphreys and Pearce (1981) who showed sub-tidal currents of this order both from tidally averaged current meter observations and from their more complex numerical model. The effect of river outflow on Penobscot Bay circulation could not adequately be considered with this model.

It appears as though both tidally induced residuals and wind driven flows are equally important in defining the non time-dependent circulation in Penobscot Bay. These two forcings did, however, generate currents of a different nature. The wind stress generated currents which formed an overall circulation pattern in the bay whereas the tidally induced residuals were localized to near shore areas. Since the tidally induced residuals are localized, it is expected that they would be harder to resolve with a drifter study, so it is not surprising that evidence of such flow was not seen in the drifter data. The wind driven currents were shown to be sensitive to the direction of the wind. General trends are in agreement both with the observations in this study and other observations, and the predicted features make sense in accordance with the model dynamics.

CONCLUSIONS:

This study presents an overview of what is already known about the physical oceanography of Penobscot Bay as well as the results of an observational study and a numerical model. A first order picture of the hydrography of the bay was assimilated from observational data collected both for this project and for other studies. This showed that Penobscot Bay varies from a moderately stratified estuary to a well-mixed estuary depending on season and location in the bay. No definitive circulation pattern in the bay was presented in the literature, nor did the observations provide any concrete evidence of such. The 2-D numerical model predicted both tidal and sub-tidal currents which agreed generally with known information. However, since no comprehensive and numerical comparison of the model to observations was possible, the predictions must not be viewed as definitive. The model did incorporate several assumptions and simplifications which could lead to error in the final results.

The model predictions did yield interesting information about the currents, providing a picture of the M2 barotropic tide as well as sub-tidal currents arising from tidally averaged vorticity flux, wind stress, and river outflow. The tidal picture agreed with the general estuarine pattern of greater sea surface displacement at the head of the bay and greater velocities towards the mouth. River driven outflow was not able to be adequately considered with the model. Both wind driven currents and tidal residuals were shown to be of the same order of magnitude and to create a significant sub-tidal circulation.

The information presented within can be used to aid in further studies of the complex oceanographic features of Penobscot Bay. As in all estuaries, the interaction between the physical, biological, and chemical systems is of vital importance to the well being of Penobscot Bay. This study provides an initial picture of the physical aspects. Unfortunately, Penobscot Bay has been subjected to much pollution and an understanding of the tidal and sub-tidal currents in the bay can help in controlling this pollution and predicting the damage that might be done. The local economy is deeply rooted in the bay, and with a greater scientific understanding of the bay, the economy can continue to be supported in a healthy way.

Acknowledgements

I would like to thank Jonathan Sharp and Kuo Wong at the University of Delaware whose support through the REU program at the College of Marine Studies made the field study possible. My advisor, Philip Bogden, also deserves special thanks for guiding me throughout the past year. This project could not have been undertaken successfully without the help, support, and trust of the following individuals: Carol Janzen, Tammy Schirmer, Devens and Jerrie Hamlen, David Weaver, Robert, Whitney, the Ladd family, Dr. Charles Yentsch, and Doug Phinney.

References Cited

Csanady, G.T., Circulation in the Coastal Ocean, D. Reidel Publishing Company, Boston, 1982.

Davis, Russ E., "Drifter Observations of Coastal Surface Currents During CODE: The Method and Descriptive View", *Journal of Geophysical Research*, May 20, 1985, 4741-4755.

Haefner Jr., P.A., "Hydrography of the Penobscot Bay River (Maine) Estuary", *Journal of Fisheries Research Board of Canada,* 24(7), 1553-1571, 1967.

Humphreys III, A.C. and B.R. Pearce, "Currents in Penobscot Bay, Maine", *in* Oceans 81--Conference Record of *The Ocean-An International Workplace*, Boston, pp. 805-809, 1981.

Kenefick, Andrew M., "Barotropic M2 Tides and Tidal Currents in Long Island Sound: A Numerical Model", *Journal of Coastal Oceanography*, 1(2), 117-128, 1985.

Kundu, Pijush K., Fluid Mechanics, Academic Press, Inc., San Diego, 1990.

Menke, W., Geophysical Data Analysis: Discrete Inverse Theory, Academic Press Inc., Orlando, 1984.

Mesinger, F. and A. Arakawa, Numerical Methods Used in Atmospheric Models, GARP Publication Series, No. 17, Volume I, 63 pp., 1976.

Normandeau Associates Inc., "Environmental Survey of Upper Penobscot Bay, Maine. Second Quarterly Report for Central Maine Power Company", 385 pp. 1975.

Normandeau Associates Inc., "An Oil Pollution Prevention Abatement and Management Study For Penobscot Bay, Maine", Vol. II, 1978.

Officer, Charles B., The Physical Oceanography of Estuaries (and Associated Coastal Waters), Wiley and Sons, New York, 1976.

Pickard, G.L. and W.J. Emery, Descriptive Physical Oceanography, Pergamon Press, Oxford, 4th Edition, 1982.

Pond, S. and Pickard, G.L., Introduction to Dynamical Oceanography, Pergamon Press, Oxford, 1983.

Taylor, G.I., "Tidal Friction in the Irish Sea", Philosophical Transactions, pp. 1-33, 1919.

Zimmerman, J.T.F., "Dynamics, Diffusion, and Geomorphological Significance of Tidal Residual Eddies", *Nature*, Vol. 290, April 16, 1981.

APPENDIX A: ANALYTIC CHECK OF MODEL

An analytic check of the model was performed in the preliminary stages to make sure that the model was predicting correctly. This simplified case was for a one dimensional channel with a closed end and tidal open boundary forcing. This problem is set up in more detail in Officer (1976). Officer states that the solution to the problem is of the form:

$$h = ae^{-\mu x}\cos(\omega t - kx) + ae^{\mu x}\cos(\omega t + kx) \tag{A.1}$$

which specifies two waves traveling in opposite directions, one decaying to the right and the other decaying to the left. a is the amplitude of the waves, x is the distance into the channel, ω is the frequency, k is the wave number, and $\mu = \beta/2\sqrt{gH}$ where β is the friction coefficient which is commonly assigned a value of .001 m/s. The tidally forced open boundary condition is specified as follows:

$$h = a_o\cos(\omega t) \quad \text{at} \quad x = L \tag{A.2}$$

where L is the open boundary. Plugging in this boundary condition and converting to exponential form, we get

$$a_o = \mathrm{Re}\left[a\left(e^{-(\mu+ik)L} + e^{(\mu+ik)L}\right)\right] \tag{A.3}$$

assuming that a is real. With the use of a trigonometric identity, this becomes

$$a_o = \mathrm{Re}\left[2a\cosh(\mu L + ikL)\right] \tag{A.4}$$

Using another trigonometric identity and solving for a, we get

$$a = \frac{a_o}{2\cosh(\mu L)\cos(kL)} \tag{A.5}$$

Plugging this back into equation A.1, the final solution becomes

$$h = \frac{a_o}{2\cosh(\mu L)\cos(kL)}\left[e^{-\mu x}\cos(\omega t - kx) + e^{\mu x}\cos(\omega t + kx)\right] \tag{A.6}$$

This solution was checked with the numerical model for the same set up and the agreement was good. There were errors introduced by the finite-difference method of approximating the partials, but the solutions were close enough to check the model's accuracy.

APPENDIX B: CODE FOR NUMERICAL MODEL

```
 /*This is the C-code written to solve the tidal model.  The code for
    the three residual models is very similar to this code.  The only
    differences are in boundary conditions and one term in the equations
    used to calculate U and V.  Therefore, this code is not included here.
 */

/* include files*/

#include <stdio.h>
#include <stdlib.h>
#include <math.h>

/*define constants*/

#define TIME_STEP 10.0
#define END_TIME 500000
#define SPACE_STEP 800.0
#define X_GRIDS 42
#define Y_GRIDS 65
#define g 9.81
#define SIDE_BC 0.0
#define R .001
#define AMPLITUDE 2
#define PI 3.141592654
#define PERIOD 44640.0
#define f 0.0001
#define LAND_FLAG 0

/*global arrays*/

double uarray[3][X_GRIDS][Y_GRIDS];     /*holds full grid of values for n-1,n,and n+1*
double varray[3][X_GRIDS][Y_GRIDS];
double harray[3][X_GRIDS][Y_GRIDS];
float darray[X_GRIDS][Y_GRIDS];         /*array of bathymetry data*/
float uprimearray[X_GRIDS][Y_GRIDS];
float vprimearray[X_GRIDS][Y_GRIDS];
double vortarray[X_GRIDS][Y_GRIDS];

/*this function initializes the u,v,h arrays to zero*/

void init_arrays()
{
    int x = 0, y = 0, z = 0;

    while(z < 2) {
        while(y < Y_GRIDS) {
            while(x < X_GRIDS) {
                harray[z][x][y] = 0;        /*no initial sea surface displacement*/
                x++;
```

```
            }
            x=0;
            y++;
        }
        y=0;
        z++;
    }
    y=0;
    z=0;

    while(z < 2) {
        while(y < Y_GRIDS) {
            while(x < X_GRIDS) {
                uarray[z][x][y] = 0;        /*no initial u velocity*/
                x++;
            }
            x=0;
            y++;
        }
        y=0;
        z++;
    }
    y=0;
    z=0;

    while(z < 2) {
        while(y < Y_GRIDS) {
            while(x < X_GRIDS) {
                varray[z][x][y] = 0;        /*no initial v velocity*/
                x++;
            }
            x=0;
            y++;
        }
        y=0;
        z++;
    }
    y=0;
    x=0;
}

/*loads depth values into array from bathymetry file 'h2.dat'*/

void load_depth_array(void)
{
    float temp;
    int x=0, y=0;
    FILE *input, *output;


    if ((input = fopen("h2.dat", "r")) == NULL)
        printf("Unable to open matrix2.dat!");
```

```
    while (y < Y_GRIDS) {                    /*put depth values into darray*/
        while(x < X_GRIDS) {
              fscanf(input, "%f", &temp);
              if(temp!=0)
            darray[x][y] = temp;
              else
            darray[x][y] = LAND_FLAG;
              x++;
        }
        x=0;
        y++;
          }
    x=0;
    y=0;

    fclose(input);
}

/*calculates the n+1 value of u for every grid point incorporating all
    boundary conditions*/

void calculate_u (void)
{
    double ujlnp, ujlnm, hjpln, hjmln, k, height;
    int x = 0, y = 0;

    k = ((g * TIME_STEP) / SPACE_STEP);

    while(y < Y_GRIDS) {
        while (x < X_GRIDS) {
            if (darray[x][y] != LAND_FLAG) {

                ujlnm = uarray[0][x][y];

                if(x==X_GRIDS-1 || darray[x+1][y]==LAND_FLAG)    /*spatial overstep*/
                    hjpln = harray[1][x][y];
                else
                    hjpln = harray[1][x+1][y];

                if(x==0 || darray[x-1][y]==LAND_FLAG)            /*spatial understep*/
                    hjmln = harray[1][x][y];
                else
                    hjmln = harray[1][x-1][y];

                if(x==0 || x==X_GRIDS-1 ||                       /*u=0 at edges*/
                        darray[x+1][y]==LAND_FLAG || darray[x-1][y]==LAND_FLAG)
                    ujlnp = SIDE_BC;
                else
                    ujlnp = -k*(hjpln - hjmln) + ujlnm
                          + (2*TIME_STEP*f*(varray[1][x][y]))
                          - (2*TIME_STEP*(((R/darray[x][y])*(uarray[0][x][y]))));

                uarray[2][x][y] = ujlnp;
```

```
                x++;
                }
            else {                                  /*u values for land points*/
                uarray[2][x][y] = LAND_FLAG;
                x++;
                }
        }
        x=0;
        y++;
    }
}

/*does the same thing as calculate_u but for v velocities*/

void calculate_v (void)
{
    double vjlnp, vjlnm, hjlpn, hjlmn, k, height;
    int x = 0, y = 0;

    k = ((g * TIME_STEP) / SPACE_STEP);

    while(y < Y_GRIDS) {
        while (x < X_GRIDS) {
            if(darray[x][y]!=LAND_FLAG) {

                vjlnm = varray[0][x][y];

                if(y==Y_GRIDS-1 || darray[x][y+1]==LAND_FLAG)       /*spatial overstep
                    hjlpn = harray[1][x][y];
                else
                    hjlpn = harray[1][x][y+1];

                if(y==0 || darray[x][y-1]==LAND_FLAG)               /*spatial underste
                    hjlmn = harray[1][x][y];
                else
                    hjlmn = harray[1][x][y-1];

                if(y != Y_GRIDS-1 && (y==0 || darray[x][y+1]==LAND_FLAG ||
                                             darray[x][y-1]==LAND_FLAG))
                    vjlnp = SIDE_BC;                                /*v=0 at edges*/
                else
                     vjlnp = -k*(hjlpn - hjlmn) + vjlnm
                         -(2*TIME_STEP*f*(uarray[1][x][y]))
                     -(2*TIME_STEP*(((R/darray[x][y])*(varray[0][x][y]))));

                varray[2][x][y] = vjlnp;
                x++;
            }
            else {                                  /*v values for land points*/
                varray[2][x][y] = LAND_FLAG;
                x++;
                }
        }
```

```
        x=0;
        y++;
    }
}

/*calculates sea surface displacement values fo every grid point for n+1 time step*/

void calculate_h (void)
{
    double hjlnp, hjlnm, ujpln, ujmln, vjlpn, vjlmn,
                         djpln, djmln, djlpn, djlmn, k, height, depth;
    int x = 0, y = 0;

    while(y < Y_GRIDS) {
        while (x < X_GRIDS) {
            if(darray[x][y]!=LAND_FLAG) {
                k = (( TIME_STEP) /( SPACE_STEP));

                hjlnm = harray[0][x][y];

                if(x==X_GRIDS-1 || darray[x+1][y]==LAND_FLAG){
                    ujpln = uarray[1][x][y];
                    }
                else{
                    ujpln = uarray[1][x+1][y];
                    }

                if(x==0 || darray[x-1][y]==LAND_FLAG){
                    ujmln = uarray[1][x][y];
                      }
                else{
                    ujmln = uarray[1][x-1][y];
                      }

                if(y==Y_GRIDS-1 || darray[x][y+1]==LAND_FLAG){
                    vjlpn = varray[1][x][y];
                      }
                else{
                    vjlpn = varray[1][x][y+1];
                      }

                if(y==Y_GRIDS-1)
                  djlpn = darray[x][y];
                else
                  djlpn = darray[x][y+1];
                if(y==0)
                  djlmn = darray[x][y];
                else
                  djlmn = darray[x][y-1];
                if(x==0)
                  djmln = darray[x][y];
                else
                  djmln = darray[x-1][y];
```

```
                if(x==X_GRIDS-1)
                  djpln = darray[x][y];
                else
                  djpln = darray[x+1][y];

                if(y==0 || darray[x][y-1]==LAND_FLAG){
                    vjlmn = varray[1][x][y];
                    k=((2.0*TIME_STEP)/SPACE_STEP);
                      }
                else{
                    vjlmn = varray[1][x][y-1];
                      }

                hjlnp = -k*((djpln*ujpln - djmln*ujmln +
                             djlpn*vjlpn - djlmn*vjlmn)) + hjlnm;

                harray[2][x][y] = hjlnp;
                x++;
                }
            else {                                  /*h values for land points*/
               harray[2][x][y] = LAND_FLAG;
               x++;
               }
        }
        x = 0;
        y++;
    }
}

/* this function will calculate the vorticity of a inputted point (x,y)
   and returns the value of vorticity*/

double calculate_vorticity(int x, int y)
{
        double vjpl, vjml, ujlp, ujlm, grid_vort;

      if (x==X_GRIDS-1)                         /*x overstep*/
        vjpl = varray[1][x][y];
      else
        vjpl = varray[1][x+1][y];
      if (x==0)                                 /*x understep*/
        vjml = varray[1][x][y];
      else
        vjml = varray[1][x-1][y];
      if (y==Y_GRIDS-1)                        /*y overstep*/
        ujlp = uarray[1][x][y];
      else
        ujlp = uarray[1][x][y+1];
      if (y==0)                                 /*y understep*/
        ujlm = uarray[1][x][y];
      else
        ujlm = uarray[1][x][y-1];
```

```
      grid_vort = (vjpl - vjml - ujlp + ujlm)/(2*SPACE_STEP);
          return grid_vort;
      }

/*calculates and records vorticity at all grid points at any time*/

void calc_print_vortarray(void)
{
  int x=0, y=0;
  FILE *va;

  va = fopen("vorticity", "a");

  while(y<Y_GRIDS) {
    while(x<X_GRIDS) {
      if(darray!=LAND_FLAG)
    fprintf(va, "%e ", calculate_vorticity(x,y));
      else
    fprintf(va, "0.0 ");
      x++;
    }
    fprintf(va, "\n");
    y++;
    x=0;
  }
  fprintf(va, "\n");
  fclose(va);
}

/*calculates u forcing array to be used in tidal residual model as forcing*/

void calculate_uprime(void)
{
  int x=0,y=0;
  static int counter=0;
  counter++;

  while(y<Y_GRIDS) {
    while(x<X_GRIDS) {
      uprimearray[x][y] += (calculate_vorticity(x,y)*(uarray[1][x][y]));
      x++;
      }
    y++;
    x=0;
  }
  x=0;
  y=0;

  if(counter==4464){
    while(y<Y_GRIDS) {
      while(x<X_GRIDS){
    uprimearray[x][y]=uprimearray[x][y]/counter;
    x++;
```

```
      }
      y++;
      x=0;
    }
  }
}

/*calculates v forcing array to be used in tidal residual model as forcing*/

void calculate_vprime(void)
{
  int x=0,y=0;
  static int counter=0;
  counter++;

  while(y<Y_GRIDS) {
    while(x<X_GRIDS) {
      vprimearray[x][y] += (calculate_vorticity(x,y)*(varray[1][x][y]));
      x++;
    }
    y++;
    x=0;
  }
  x=0;
  y=0;

  if(counter==4464){
      while(y<Y_GRIDS) {
        while(x<X_GRIDS){
        vprimearray[x][y]=vprimearray[x][y]/counter;
        x++;
      }
      y++;
      x=0;
    }
  }
}

/*record forcing arrays*/

void print_prime_arrays(void)
{
  int x=0, y=0;
  FILE *up,*vp;

  up = fopen("uprime", "w");
  vp = fopen("vprime", "w");

   while(y < Y_GRIDS) {
               while (x < X_GRIDS) {
                       if(darray[x][y] != LAND_FLAG)
                               fprintf(up, "%.4e  ", uprimearray[x][y]);
                       else
```

```
                        fprintf(up, "0.0    ");
                    if(darray[x][y] != LAND_FLAG)
                        fprintf(vp, "%.4e  ", vprimearray[x][y]);
                    else
                        fprintf(vp, "0.0    ");
                    x++;
                }
                fprintf(up, "\n");
                fprintf(vp, "\n");
                x=0;
                y++;
            }
    fclose(vp);
    fclose(up);
}

/*this function performs a five point weighted average on u,v,and h arrays
    in order to combat grid point oscillation*/

void smooth_arrays()
{
    double hxpy, hxmy, hxyp, hxym,
           uxpy, uxmy, uxyp, uxym,
           vxpy, vxmy, vxyp, vxym;
    int x=0, y=0;

    while(y<Y_GRIDS-1){
      while(x<X_GRIDS){
        if(darray[x][y]!=LAND_FLAG){
      if(y==Y_GRIDS-1 || darray[x][y+1]==LAND_FLAG){
        hxyp = harray[0][x][y];
        uxyp = uarray[0][x][y];
        vxyp = varray[0][x][y];
      }
      else {
        hxyp = harray[0][x][y+1];
        uxyp = uarray[0][x][y+1];
        vxyp = varray[0][x][y+1];
      }
          if(y==0 || darray[x][y-1]==LAND_FLAG){
        hxym = harray[0][x][y];
        uxym = uarray[0][x][y];
        vxym = varray[0][x][y];
      }
      else{
        hxym = harray[0][x][y-1];
        uxym = uarray[0][x][y-1];
        vxym = varray[0][x][y-1];
      }
          if(x==X_GRIDS-1 || darray[x+1][y]==LAND_FLAG){
        hxpy = harray[0][x][y];
        uxpy = uarray[0][x][y];
        vxpy = varray[0][x][y];
```

```
    }
    else{
      hxpy = harray[0][x+1][y];
      uxpy = uarray[0][x+1][y];
      vxpy = varray[0][x+1][y];
    }
        if(x==0 || darray[x-1][y]==LAND_FLAG){
      hxmy = harray[0][x][y];
      uxmy = uarray[0][x][y];
      vxmy = varray[0][x][y];
    }
    else{
      hxmy = harray[0][x-1][y];
      uxmy = uarray[0][x-1][y];
      vxmy = varray[0][x-1][y];
    }

    harray[0][x][y] = ((hxpy+hxmy+hxyp+hxym)/8.0) + harray[0][x][y]/2.0;
    uarray[0][x][y] = ((uxpy+uxmy+uxyp+uxym)/8.0) + uarray[0][x][y]/2.0;
    varray[0][x][y] = ((vxpy+vxmy+vxyp+vxym)/8.0) + varray[0][x][y]/2.0;
    x++;
      }
      else
        x++;
    }
    y++;
    x=0;
  }
}

/*this function introduces the tidal forcing at th open boundary*/

void modify_height(double time)
{
    double q = 0;
    int x=0;

    q = (((2*PI)/PERIOD) * time);

    while(x<X_GRIDS) {                              /*open boundary at bottom edge*/
        harray[1][x][Y_GRIDS-1] = (AMPLITUDE*(cos(q)));
        x++;
    }
}

/*prints u,v,h arrays to file*/

void print_arrays(FILE *uf, FILE *vf, FILE *hf)
{
    int x=0,y=0;

    while(y < Y_GRIDS) {
        while (x < X_GRIDS) {
```

```
            if(darray[x][y] != LAND_FLAG)
                fprintf(uf, "%.4lf  ", uarray[1][x][y]);
            else
                fprintf(uf, "0.0    ");
            if(darray[x][y] != LAND_FLAG)
                fprintf(vf, "%.4lf  ", varray[1][x][y]);
            else
                fprintf(vf, "0.0    ");
            if(darray[x][y] != LAND_FLAG)
                fprintf(hf, "%.4lf  ", harray[1][x][y]);
            else
                fprintf(hf, "0.0    ");
            x++;
        }
        fprintf(uf, "\n");
        fprintf(vf, "\n");
        fprintf(hf, "\n");
        y++;
        x=0;
    }
    fprintf(uf, "\n");
    fprintf(vf, "\n");
    fprintf(hf, "\n");
}

/*shifts each array to previous time step so as to calculate
     the next time step*/

void shift_arrays(void)
{
    int x = 0, y = 0;

    while(y < Y_GRIDS) {
        while (x < X_GRIDS) {
            uarray[0][x][y] = uarray[1][x][y];
            uarray[1][x][y] = uarray[2][x][y];
            varray[0][x][y] = varray[1][x][y];
            varray[1][x][y] = varray[2][x][y];
            harray[0][x][y] = harray[1][x][y];
            harray[1][x][y] = harray[2][x][y];
            x++;
        }
        x = 0;
        y++;
    }
}

/*the main function performs the time stepping of the model.  It makes
    iterative calls to the various functions until END_TIME is reached*/

void main(void)
{
    long int s = 0, mod;
```

```
    double t = 0;
    FILE *uf, *hf, *vf;

    init_arrays();
    load_depth_array();
    mod = PERIOD/TIME_STEP;

    if ((vf = fopen("vnew4", "w")) == NULL)
        printf("Unable to open vfile2!!\n");

    if ((uf = fopen("unew4", "w")) == NULL)
        printf("Unable to open ufile2!!\n");

    if ((hf = fopen("hnew4", "w")) == NULL)
        printf("Unable to open hfile2!!\n");

    while(t <= END_TIME) {                          /*main loop*/
       modify_height(t);
       calculate_u();
       calculate_v();
       calculate_h();
       if(s%10==0){
         smooth_arrays();
       }

       if(s==44640 ||
          s==45198 ||          /*record arrays every 1/8th tidal cycle*/
          s==45756 ||         /*in the last one to see evolution of flow field*/
          s==46314 ||
          s==46872 ||
          s==47430 ||
          s==47988 ||
          s==48546) {
            print_arrays(uf, vf, hf);
            printf("%.2f\ntime=%f\n",harray[1][0][Y_GRIDS-1], t);
            calc_print_vortarray();
        }

       if(t>=(PERIOD*10) && t<(PERIOD*11)) {
         calculate_uprime();
         calculate_vprime();
       }

        shift_arrays();
        t += TIME_STEP;
        s++;
    }
    print_prime_arrays();
    fclose(uf);
    fclose(hf);
    fclose(vf);
}
```